Addis Ababa University

Addis Ababa Institute of Technology

School of Electrical and Computer Engineering

Design of Improved TEM Horn Antenna in Double Exponential Approach for Impulse GPR Applications

by

Zekarias Afework

Advisor

Dr. Ephrem Teshale

A Thesis Submitted to the School of Graduate Studies of Addis Ababa University in Partial Fulfillment of the Requirements for the Degree of **Master of Science** in **Electrical Engineering** (***Communication Stream***)

May, 2021

Addis Ababa, Ethiopia

Addis Ababa University

Addis Ababa Institute of Technology

School of Electrical and Computer Engineering

Design of Improved TEM Horn Antenna in Double Exponential Approach for Impulse GPR Applications

Zekarias Afework

Approval by Board of Examiners

_____	_____
Chairman, School Graduate Committee	Signature
Dr. Ephrem Teshale	_____
Advisor	Signature
_____	_____
Internal Examiner	Signature
_____	_____
External Examiner	Signature

Declaration

I, the undersigned, declare that this thesis is my original work, has not been presented for a degree in this or any other university, and all sources of materials used for the thesis have been fully acknowledged.

Zekarias Afework _____

Name Signature

Place: Addis Ababa

Date of Submission: _____

This thesis has been submitted for examination with my approval as a university advisor.

Dr. Ephrem Teshale _____

Advisor's Name Signature

ABSTRACT

Ground Penetrating Radar (GPR) is a popular geophysical technique that is used to investigate the ground using electromagnetic waves. Analogous to medical imaging GPR is used for subsurface imaging and exploration.

Antenna is a key element of any GPR system. The design of GPR antennas differs from the classical approach. Classical antennas are designed for operating in free space but antennas for GPR must operate in the vicinity of the ground and this is a major constraint in their design. The GPR antenna must couple the electromagnetic waves directly in to the ground.

In this thesis, improved Transverse Electromagnetic (TEM) horn antennas are designed for impulse GPR applications and improving the design of the TEM horn antenna is focused on reducing the aperture reflections in double exponential approach.

Student version of FEKO software is used in the simulation and The simulation results show that, TEM horn antennas, TEM60cm and TEM120cm each with aperture impedance of 200 and 250 Ohm designed in double exponential approach have less Voltage Standing Wave Ratio(VSWR) than TEM horn antenna with 377 Ohm aperture impedance of similar size as the frequency of operation increase and the VSWR of TEM60cm and TEM120cm each with aperture impedance of 200 and 250 Ohm is less than 2 over an ultra-wide frequency range within the frequency range of interest.

ACKNOWLEDGMENTS

First and foremost, I would like to thank the almighty, omniscient and omnipresent **God the Saviour** for giving me the perseverance to finish the thesis and without whom nothing is possible and to **Holy Mary** for her intercession.

I am grateful to Addis Ababa Institute of Technology for giving me the opportunity to pursue my M.Sc. studies.

My sincere thanks goes to my advisor Dr. Ephrem Teshale for giving me the opportunity to work with him, for his support and guidance in order to complete this thesis.

I would also like to extend my gratitude to my families, especially to my beloved father Ato Afework Yohannes Degu and my beloved mother W/ro Ethenesh Tsegaye Woldesenbet and friends who provide me valuable feedback and support throughout the course of doing this thesis.

Last but not least I would like to thank Altair University for providing me student version of FEKO simulation software free of charge and for the educational Altair FEKO student forum.

DEDICATION

This thesis is dedicated to my beloved father **Ato Afework Yohannes Degu** and to my beloved mother **W/ro Ethenesh Tsegaye Woldesenbet.**

For their endless love, support and encouragement.

TABLE OF CONTENTS

LIST OF TABLES

Table **Page**

LIST OF FIGURES

Figure **Page**

ABBREVIATIONS

3D	Three-dimensional
A/D	Analog-to-Digital converter
AAiT	Addis Ababa Institute of Technology
CEM	Comprehensive Computational Electromagnetics
CMA	Characteristic Mode Analysis
DARPA	Defense Advanced Research Projects Agency
EH Waves	Hybrid Electromagnetic Waves
EM	Electromagnetic
EMC	Electromagnetic Compatibility
EMI	Electro Magnetic Interference
FCC	Federal Communications Commission of United States of America
FDTD	Finite Difference Time Domain
FEKO	FEldberechnung bei Körpern mit beliebiger Oberfläche
FEM	Finite Element Method
GPR	Ground Penetrating Radar
GPS	Global Positioning System
HE Waves	Hybrid Electromagnetic Waves
IEEE	Institute of Electrical and Electronics Engineers
LE-PO	Large Element Physical Optics
LNA	Low Noise Amplifier
LPDA	Log-Periodic Dipole Antennas
MLFMM	Multilevel Fast Multipole Method
MoM	Method of Moments
NDT	Non Destructive Testing
PCs	Personal Computers

PEC	Perfect Electric Conductor
PO	Physical Optics
PRF	Pulse Repetition Frequency
RCS	Calculation of Scattering
RF	Radio Frequency
RL-GO	Ray Launching Geometrical Optics
Rx	Receiver
S/H	Sample and Hold circuit
SRD	Step Recovery Diodes
Std	Standard
TE	Transverse Electric
TEM	Transverse Electromagnetic
TEM120cm	Transverse Electromagnetic horn antenna with 120cm length
TEM60cm	Transverse Electromagnetic horn antenna with 60cm length
TM	Transverse Magnetic
TVG	Time-Varying Gain
Tx	Transmitter
UTD	Uniform Theory of Diffraction
UWB	Ultra-Wideband
UXO	Unexploded Ordnance
VSWR	Voltage Standing Wave Ratio

CHAPTER I

Introduction

Antennas are one of the most critical parts in ground penetrating radar (GPR) systems. They substantially determine the quality of the obtained GPR raw data. Due to the fact that GPR antennas are usually situated in the vicinity of the ground, their requirements are different from those of antennas operating in free space. Their design criteria can also vary depending on the application. More stringent antenna requirements are usually imposed on GPR for detection of small objects located near the air-ground interface, such as landmines. In the case of impulse GPR, such an application requires a transmit pulse which is short in duration to achieve adequate resolution in space. This implies that the antenna should be ultra-wideband for allowing proper transmission of the frequency components contained in the pulse spectrum [1].

The important parameters determining the system performance, such as antenna beam width and operational frequency depend on the properties of the ground. The optimal antenna design must provide steady performance for different ground types and weather conditions [2].

The desired antenna performance is to transmit and receive short duration, time domain waveforms (in the order of a few nanoseconds). The duration of the time domain antenna pulse is the trade-off between range resolution and penetration depth. The tail(See Figure 1.1.) of the antenna signal must be minimized to prevent masking of targets by the air-ground interface or nearby object reflections [2].

The class of antennas with ultra-wideband and linear phase properties is called transient-antennas. The term transient is more closely related to time domain performance.We divide the time domain antenna response in two parts; the main pulse and the tail. In the main pulse we distinguish two regions. The transient region is

resulting from the direct radiation of the excitation pulse. The resonance region is caused by reflections in the internal antenna structure (e.g. end of dipole, antenna shield).The tail is specified according some decaying law (e.g. exponential) [2].

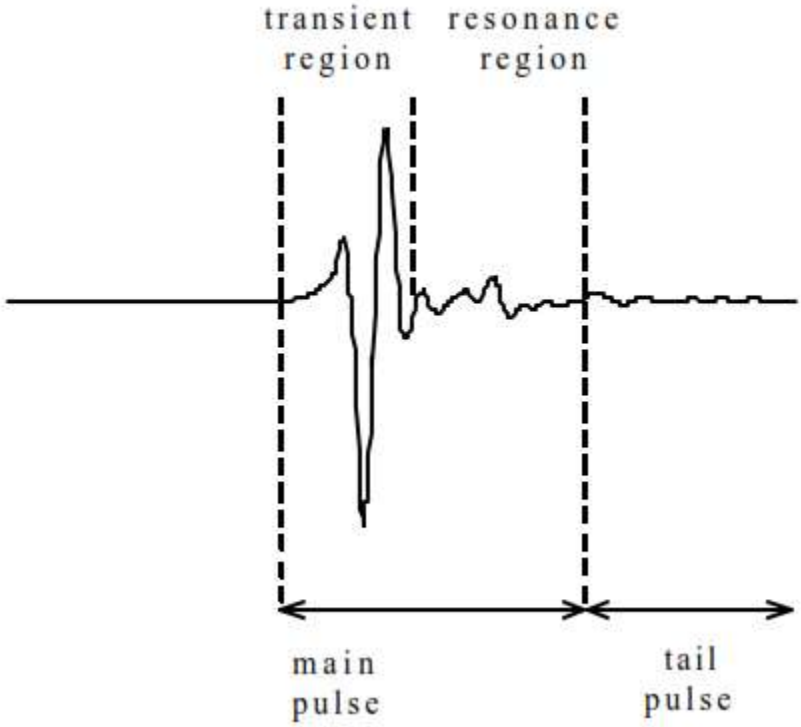

Figure 1. 1: Time domain antenna response [2]

To transmit short duration time pulses, an ultra-wideband antenna is needed. However, the bandwidth is not the only condition. A linear phase characteristic, constant phase center, constant polarization and constant gain are also required. For example, spiral and log periodic antennas have a high operational frequency range, but the time domain antenna response have a long duration. Examples of transient antenna performance are the infinite dipole antenna and TEM horn [2].

Impulse launching and receiving antennas are required for ultra-wideband applications involving high-fidelity transmitting and sensing of impulse electromagnetic fields [3].

Due to their dispersive characteristics conventional wideband antennas, such as log-periodic arrays, spiral antennas, and ridged horn type antennas, perform poorly as high-fidelity antennas for wideband impulsive waveforms [3].

However, a TEM horn forms a natural structure for low-dispersion launching and receiving of ultra-wideband impulses [3]. A TEM horn antenna provides minimum-duration response to impulsive input or output fields and is able to discriminate between events occurring in the time domain [4].

1.1 Statement of the problem

The state of the art approach in TEM horn antenna design is to set the aperture impedance to 377 Ohm in order to have best matching between the aperture and free space.

The problem in the state of the art approach is that matching the aperture impedance to free space does not assure the best matching performance so it is required to improve the design of the TEM horn antenna.

Thus, improving the design of the TEM horn antenna is focused on reducing the aperture reflections in double exponential approach (Exponential tapering has the advantage of smooth impedance variation and mathematical ease) by making the aperture impedance of the TEM horn as 200 and 250 Ohm.

1.2 Objective

1.2.1 General objective

The general objective in this thesis is to improve the design of TEM horn antennas i.e. to design TEM horn antennas in double exponential approach by making the aperture impedances of the TEM horn antennas as 200 and 250 Ohm thereby decreasing the aperture reflections.

1.2.2 Specific objectives

The specific objectives of this thesis are:

- Design and simulate improved various TEM horn antennas for impulse GPR applications.
- Compare the VSWR of various TEM horn antennas by varying the aperture impedance.

1.3 Methodology

The methodology is based on referring books, articles and literatures written on the subject.

List of major activities accomplished phase by phase in the thesis work are listed below.

- Review of books and literatures written on GPR, Ultra-Wideband(UWB) antenna and TEM horn antenna.
- Various TEM horn antenna design methods are studied.
- Drawbacks from the existing TEM horn antenna design methods are identified.
- Improved TEM horn antennas are designed.
- Study different simulation software such as COMSOL Multi-physics and FEKO then applied FEKO that is best suited for this thesis.
- Finally, the designed improved TEM horn antennas are simulated in FEKO.

1.4 Related work

In [5] Adaptive Wire Bow-Tie Antenna for GPR Applications was designed. The antenna is able to adapt its input impedance to a variation in the antenna elevation and soil type to keep reflections at the antenna's terminal minimum. As a result, energy transfer from the generator to the antenna is maximized, which in turn maximizes the energy radiated by the antenna into the ground for different antenna elevations and soil types.

In [6] a short transverse electromagnetic (TEM) horn with continuously tapered resistive loading was developed for directional reception or transmission of picosecond pulses with minimal distortion. It was found to be broadband and non-dispersive with a low VSWR.

In [7] a TEM horn antenna filled with dielectric was designed. Filling dielectric between the metal flairs in the TEM horn antenna results in concentration of electromagnetic field thus reducing the coupling, Electro Magnetic Interference (EMI) and physical size**.** But such a filling will result in increase of reflection from the antenna aperture causing increase of the antenna late-time ringing [7].

In [8] A first prototype of a dielectric filled TEM horn antenna for application in a GPR system was designed. This prototype radiates 2.2 times more energy into the sandy half space, is less sensitive to external EMI and provides 5 times smaller (in power) coupling in the antenna system, and finally is approximately two times smaller than the air filled TEM horn (designed for radiation of same pulses in free space).

A pioneer work in TEM horn antenna design is found in [9]. The equations used for the TEM horn antenna design are listed in Table-1.1. The reported VSWR of the designed antenna is less than three within the frequency range of interest. The drawback in this design work is that the aperture impedance of the TEM horn antenna was set to 377 Ohm which degraded the performance.

A TEM horn antenna was designed and manufactured based on the basis of a parallel plate waveguide theory in [10]. The equations used for the TEM horn antenna design are listed in Table-1.1. The reported VSWR of the designed antenna is less than two. The drawbacks in this design work are, the aperture impedance of the TEM horn antenna was set to 377 Ohm which degraded the performance and in addition the designed TEM horn antenna has frequency band of 75 to 1200 MHz which couldn't be applied for high frequency GPR applications.

Double exponentially tapered TEM horn antenna with a microstrip-type balun was designed and manufactured in [11]. The equations used for the TEM horn antenna design are listed in Table-1.1. The reported VSWR of the designed antenna is less than two. The drawbacks in this design work are, the aperture impedance of the TEM horn antenna was set to 377 Ohm which degraded the performance and in addition the designed TEM horn antenna has frequency band of 67.94 to 1573.9 MHz which couldn't be applied for high frequency GPR applications.

A Chebyshev tapered TEM horn antenna with improved VSWR and improved gain was designed and manufactured in [12]. The equations used for the TEM horn antenna design are listed in Table-1.1. The reported VSWR of the designed antenna is less than two. The drawbacks in this design work are, the aperture impedance of the TEM horn antenna was set to 377 Ohm which degraded the performance and difficulty in TEM horn antenna construction.

A dielectric material loaded TEM horn antenna was designed and manufactured in [13]. In [13] it was shown that match of the aperture impedance to the free space impedance does not improve but may degrade the performance. A TEM horn antenna with aperture impedance of 250 Ohm was designed and it was shown that it had lower VSWR than TEM horn with aperture impedance of 377 Ohm. The equations used for the TEM horn antenna design are listed in Table-1.1. The reported VSWR of the designed

antenna is less than two. The drawbacks in this design work are setting the aperture impedance to 250 Ohm to get the best matching performance for all antennas with different lengths and in addition difficulty in TEM horn antenna construction.

TEM horn antennas with aperture impedance of 200 to 400 Ohm were designed in [14]. It was found that the TEM horn antenna can obtain the best performance with aperture impedance of 200 Ohm. The equations used for the TEM horn antenna design are listed in Table-1.1. In [14] it was reported that there was no huge difference of performance between TEM horn antennas of different aperture impedances from 200 to 400. The drawbacks in this design work are, setting aperture impedance to 200 Ohm to get the best matching performance for all antennas with different lengths and in addition difficulty in TEM horn antenna construction.

Table 1. 1: Literature Review of TEM horn antenna design Equations

Item #	Researchers	Equations used to calculate impedance variation along the TEM	Equations used to calculate spacing between TEM upper and lower conductor	Equations used to calculate width along the TEM	Drawbacks
1	[9]	$Z_x = \sqrt{Z_{IN} Z_L}$	$y = \beta\ e^{\alpha x}$	$Z_0 = \frac{377}{(w/h)+2}$, $(w/h) \geq 1$ $Z_0 = 138\log\frac{8}{(w/h)}$, $(w/h) \leq 1$	(i) Aperture impedance was set to 377 Ohm. => But 377 Ohm is not the best aperture impedance for TEM horn antenna matching to free space. (ii) Higher VSWR up to 3.
2	[10]	$Z(y) = Z_0 e^{\alpha y}$	$d(y) = 2\{ae^{by} + c\}$	$Z(y) = \frac{d(y)}{w(y)}\eta$	(i) Aperture impedance was set to 377 Ohm. => But 377 Ohm is not the best aperture impedance for TEM horn antenna matching to free space. (ii) Limited to low frequency applications (75 to 1200 MHz).
3	[11]	$Z(y) = Z_0 e^{\alpha y}$	$d(y) = 2\{ae^{by}\}$	$Z(y) = \frac{d(y)}{w(y)}120\pi$	(i) Aperture impedance was set to 377 Ohm. => But 377 Ohm is not the best aperture impedance for TEM horn antenna matching to free space. (ii) Limited to low frequency applications (67.94 to 1573.9 MHz).
4	[12]	See Eq.1	$d(x) = \alpha e^{(\beta x)}$	$w(x) = \eta\ d(x)/Z(x)$	(i) Aperture impedance was set to 377 Ohm. => But 377 Ohm is not the best aperture impedance for

					TEM horn antenna matching to free space. (ii) Difficult in construction due to complex design.
5	[13]	See Eq.2	$y(z) = b_{line} + \frac{b - b_{line}}{d} z$ $y(z) = b_{line} \exp\left[\frac{1}{d} Ln\left(\frac{b}{b_{line}}\right) z\right]$	$Z_0(z) = \frac{\pi \eta}{\pi w + 1 + Ln(2\pi[w + 0.94])}$	(i) Aperture impedance was set to 250 Ohm. => But 250 Ohm is not the best aperture impedance for TEM horn matching to free space,the VSWR could be further improved i.e. TEM60cm with 200 Ohm aperture impedance has lower VSWR than TEM60cm with 250 Ohm aperture impedance as frequency increase. (ii) Difficult in construction due to complex design.
6	[14]	See Eq.3 (Hecken's eq.)	Linear taper	$\frac{w}{d} = \frac{8.e^A}{e^{2A} - 2}, w/d < 2$ See Eq.4	(i) Aperture impedance was set to 200 Ohm. => But 200 Ohm is not the best aperture impedance for TEM horn matching to free space, the VSWR could be further improved i.e. TEM120cm with 250 Ohm aperture impedance has lower VSWR than TEM120cm with 200 Ohm aperture impedance as frequency increase. (ii) Difficult in construction due to complex design.

Eq.1: $\ln \bar{Z} = \left(\frac{p}{2\pi} + \frac{1}{2} - \frac{p}{2\pi \cosh \pi\mu_0}\right) \ln \bar{Z}_L + \frac{\ln \bar{Z}_L}{\pi \cosh \pi\mu_0} \sum_{n=1}^{\infty} \frac{\cos \pi\sqrt{n^2 - {\mu_0}^2 - \cos n\pi}}{n} \sin np$

Where, $\bar{Z}$ is the normalized impedance at each point, $\bar{Z}_L$ is the normalized load impedance which in this case is the intrinsic impedance of free space(377 Ω),Z_0 is the characteristic impedance (100 Ω) of the feed line,$\pi\mu_0 = \beta_0 L, \pi\mu = \beta L, p = 2\pi \frac{x - L/2}{L}$, where $-\pi < p < \pi$ and L is the taper length.

Eq.2: $\ln \frac{Z_0(z)}{Z_0(0)} = \frac{1}{2} \ln \frac{Z_0(d)}{Z_0(0)} \left\{1 + G\left[B, 2\left(\frac{z}{d} - 0.5\right)\right]\right\}, 0 \le z \le d$

Where $G(B, \xi)$ is defined and tabulated for some typical values of B and ξ.

Eq.3: $Z_m = \boldsymbol{exp}[\ln(Z_b Z_a)/2 + \gamma_0 B_\varphi(2m/N - 1, B)/\sinh(B)]$

Where,$\Gamma_0 = (Z_b - Z_a)/(Z_b + Z_a), \gamma_0 = \ln(Z_b/Z_a)/2$

$\text{ø}(\text{x}, \text{A}) = \int_0^{\text{x}} \text{I}_1\left(\text{A}\sqrt{1 - \text{y}^2}\right)/\left(\text{A}\sqrt{1 - \text{y}^2}\right) \text{dy}, \varphi(\text{x}, \text{B}) = \int_0^{\text{x}} \text{I}_0\left(\text{B}\sqrt{1 - \text{y}^2}\right) \text{dy}$ and N is the *number of steps.*

Eq.4: $\frac{\text{w}}{\text{d}} = \frac{2}{\pi} \left[B - 1 - \ln(2B - 1) + \frac{\varepsilon_r - 1}{2\varepsilon_r}\left\{\ln(B - 1) + 0.39 - \frac{0.61}{\varepsilon_r}\right\}\right], w/d > 2$

In which, $A = \frac{Z_0}{60}\sqrt{\frac{\varepsilon_r + 1}{2}} + \frac{\varepsilon_r - 1}{\varepsilon_r + 1}\left(0.23 + \frac{0.11}{\varepsilon_r}\right), B = \frac{377\pi}{2Z_0\sqrt{\varepsilon_r}}$

1.5 Scope and Limitation

1.5.1 Scope of the thesis

The scope of the thesis covers the design, simulation and VSWR analysis of TEM120cm and TEM60cm with 200,250 and 377 Ohm aperture impedances.

1.6 Limitation of the thesis

The thesis is entirely based on simulation i.e. the TEM horn antennas are not manufactured so actual measurements are not made.

1.7 Contribution

The contribution of this thesis is in improving the design of the TEM horn antenna by reducing the aperture reflections (reducing VSWR) via double exponential approach by making the aperture impedance of the TEM horn as 200 and 250 Ohm and the length of the TEM horn antennas is 60 cm and 120 cm.

1.8 Thesis Layout

The thesis is highly organized in such a way that it gives a clear flow and understanding of the subject matter. The second chapter deals with GPR, the third chapter briefly deals with antennas and UWB antennas, the fourth chapter deals with TEM horn antennas, and in the fifth chapter improved TEM horn antennas are designed, The sixth chapter gives VSWR simulation of different TEM horns and the seventh chapter gives conclusions and recommendations for future works.

Finally, the wave equation, FEKO and detailed steps of designing TEM120cm with 200 Ohm aperture impedance are explained in Appendix A, B and C respectively.

CHAPTER II

Ground Penetrating Radar

2.1 GPR Introduction

Ground Penetrating Radar (GPR) is a well-accepted geophysical technique that is used to image the subsurface [15].

A typical ground penetrating radar transmits a short pulse of electromagnetic energy of 1 ns (10^{-9} s) time duration from a transmit antenna into the material. Energy reflected from discontinuities in dielectric constant, meaning when there is a difference in dielectric constant of materials in the ground, electromagnetic energy is reflected back and is received by means of a receive antenna and is then suitably processed and displayed by a radar receiver and display unit. If the transmit and receive antennas are moved at a constant velocity along a linear path, a cross-sectional image of the material can be generated. Alternatively, if the antennas are scanned in a regular grid pattern, a three-dimensional image of the target can be derived [16].

In its earliest inception, GPR was primarily applied to natural geologic materials. Now GPR is equally well applied to a host of other media such as wood, concrete, and asphalt [15].

The existence of numerous lossy dielectric material environments combined with the broad radio frequency spectrum leads to a wide range of GPR applications. The same methodology can be applied to glaciology and to nondestructive testing of concrete structures; the spatial scale of applications varies from kilometers to centimeters [15].

The most common form of GPR measurements deploys a transmitter and a receiver in a fixed geometry, which are moved over the surface to detect reflections from subsurface features. In some applications, transillumination of the volume under

investigation is more useful. Both concepts are depicted in Figure 2.1 [15]. An example of GPR response is shown in Figure 2.2 [15].

GPR allows us to detect what lies beneath the ground or within buildings. It is primarily a safety aide since it is used to prevent potentially dangerous situations arising or for the detection and treatment of hidden problems. As such, it has a wide remit whether this is the accurate location of pipes and cables in order to prevent damage during site development, the detection of crevasses in glaciers or the internal structural investigation of roads, bridges, airports, and historic buildings to detect problems before they become critical [17].

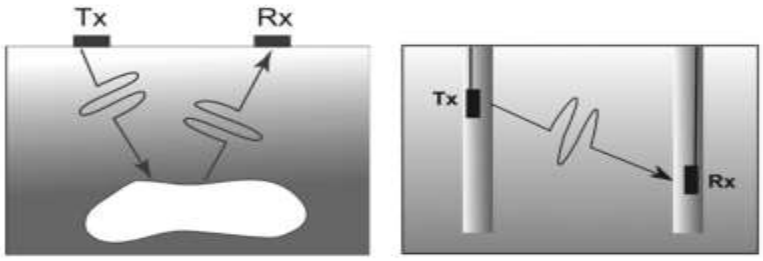

Figure 2. 1: Two modes of measurement in GPR [15].

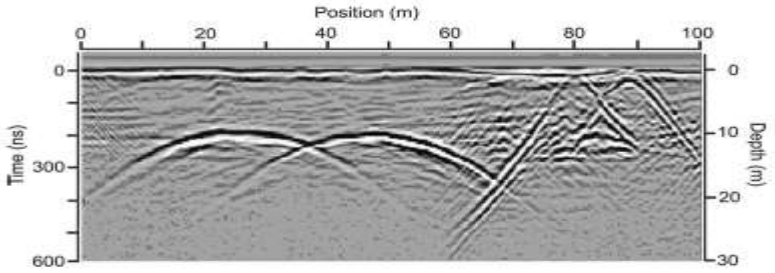

Figure 2. 2: GPR cross section obtained with a 50-MHz system traversing over two road tunnels [15].

GPR has found a secure home in the field of NDT (Non Destructive Testing). GPR is a useful technology that can look inside historic structures to discover cracks, deterioration, and weathering of internal construction supports that are keeping these buildings together [18].

2.2 Basic elements of a GPR system

Every GPR is made up of a control system, at least one transmitter antenna, at least one receiver antenna, and some means of data storage (Figure 2.3) [17].

As it is not yet possible to procure sufficiently fast transmit-receive switches with adequate performance when operating in the nanosecond time region, separate antennas for transmission and reception are needed in order to protect the receiver from the high level of transmitted signal [16].

A transmitter antenna and receiver antenna together is termed a transducer pair. It is also usual to have a viewing system for monitoring the data in real time, either a laptop, a notebook or other computing device, a data logger, or a similar type of screen if the computing device is built in. Many systems also contain a distance measurement device, typically an odometer (or encoder) wheel. Some systems use GPS (Global Positioning System) instead of a wheel [17].

Figure 2. 3: The basic elements of a GPR system [17].

From Figure-2.3: 1, controller; 2, transmitter antenna; 3, receiver antenna; 4 and 5, laptop for data storage and monitoring; and 6, encoder wheel for distance measurement [17].

The GPR controller generates electromagnetic pulses which are passed into a transmitter which then transmits into the survey medium (the soil or other material under investigation, e.g., concrete). As the signal passes through this material, parts of the signal are returned to the receiver. It is the changing nature of the buried material in the subsurface that triggers each of these reflections. The returned signals carry information back through the receiver to the controller and from there to the laptop, tablet, or other viewing device. This information is not optical and the radar does not give a picture of what lies in the subsurface, at least not in the traditional meaning of the word,the returned signal indicates that there is a material with different dielectric constant in contrast to the surrounding environment[17].

The survey medium depends on the environment under investigation. For GPR this is most commonly the ground, either open soil or man-made substances such as asphalt and concrete. It can also mean walls, ceilings and floors of buildings, ice, and any other substance within which lie targets to be investigated [17].

One of the major advantages of GPR is that it responds to any material and is not limited, for example, to metal detection. Provided that the material for which a search is being made is different in electrical and magnetic response to its surrounding environment, it can potentially be detected by a GPR. So, for example, it is perfectly possible to detect buried plastic pipes by using a GPR [17].

Laptops, data loggers, tablets, and PCs are used to set the controller's survey parameters (e.g., probing depth, frequency of sampling, number of antennas) and also the on-screen display settings which are for the benefit of the person viewing the data as these are collected [17].

2.3 GPR basic principles

2.3.1 Overview

A ground penetrating radar is an example of an ultra-wideband radar and operates in a way very similar to that of conventional radar but with several important differences. The first is that, whereas conventional radar operates over ranges of tens or hundreds of kilometres, a typical ground penetrating radar operates at ranges of a few metres and a maximum of tens of metres. The second is that the resolution of conventional radar can be tens of metres, whereas a ground-probing radar requires a resolution of some tens of centimeters or less. The final, and most important, difference is that conventional radar transmits through the air, which usually causes little attenuation, whereas ground-probing radar uses a material such as soil or concrete as a transmission medium, the attenuation of which is very high and in many cases limits the overall performance [16].

GPR can be designed to work in time or frequency domain. A GPR that operates in time domain (the so-called impulse GPR) makes use of short transient pulses as the probing signals. A GPR that operates in frequency domain utilizes a frequency-hopping technique, in which narrow-band signals are transmitted sequentially over a period of time covering in total an ultra-wide frequency band. The antenna requirements for impulse GPR are generally more stringent than for frequency-domain GPR. For impulse GPR one should select the antennas which are able to transmit short pulses properly. In frequency-domain GPR the antenna can be calibrated in the signal processing, which makes the antenna selection easier [19].

Most ground penetrating radars are time-domain, impulse systems and radiate a wavelet which approximates to a single cycle of a sinusoidal waveform. Viewed in the frequency domain the energy is spread over a wide spectrum in lines whose spectral

separation is related to the pulse repetition interval and whose envelope is related to the Fourier transform of the wavelet convolved with the transfer function of the antenna [16].

A ground penetrating radar generates a short impulse of electromagnetic energy of a few nanoseconds duration at a peak power of typically 50 W and a repetition frequency of up to 1 MHz. This impulse is then launched into the transmission medium by means of an antenna. Reflected energy from the target is gathered by means of a receiving antenna (usually similar to the transmitting antenna). The receiver processes the information by sampling, filtering and displaying the signal in a suitable form for the operator. If both antennas are scanned over the surface of the host material at a constant velocity along a linear path, a cross-sectional image of the material can be generated. If the antennas are scanned in a regular grid pattern a three-dimensional image of the volume scanned can be derived [16]. Figure 2.4 which shows a block diagram of a typical GPR system.

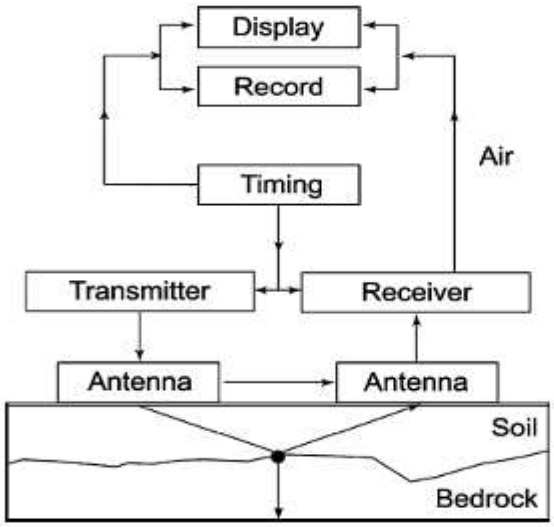

Figure 2. 4: Block diagram depicting a GPR system [15].

2.3.2 Maxwell's equations

The foundations of GPR lie in electromagnetic (EM) theory. The history of this field spans more than two centuries. Maxwell's equations mathematically describe the physics of EM fields, while constitutive relationships quantify material properties. Combining the two provides the foundations for quantitatively describing GPR signals [15].In mathematical terms, EM fields and relationships are expressed as follows [15].

$$\overline{\nabla} \times \overline{E} = -\frac{\partial \overline{B}}{\partial t} \tag{2.1}$$

$$\overline{\nabla} \times \overline{H} = \overline{J} + \frac{\partial \overline{D}}{\partial t} \tag{2.2}$$

$$\overline{\nabla} \cdot \overline{D} = q \tag{2.3}$$

$$\overline{\nabla} \cdot \overline{B} = 0 \tag{2.4}$$

Where $\overline{E}$ is the electric field strength vector (V/m); q is the electric charge density (C/m^3): $\overline{B}$ is the magnetic flux density vector (T); $\overline{J}$ is the electric current density vector (A/m^2); $\overline{D}$ is the electric displacement vector (C/m^2); t is time (s); and $\overline{H}$ is the magnetic field intensity (A/m).

2.3.3 Constitutive equations

Constitutive relationships are the means of describing a material's response to EM fields. For GPR, the electrical and magnetic properties are of importance. Constitutive equations (Equations (2.5), (2.6) and (2.7)) provide a macroscopic (or average behavior) description of how electrons, atoms, and molecules respond en masse to the application of an EM field [15].

$$\overline{J} = \tilde{\sigma}\,\overline{E} \tag{2.5}$$

$$\overline{D} = \tilde{\varepsilon}\,\overline{E} \tag{2.6}$$

$$\overline{B} = \tilde{\mu}\,\overline{H} \tag{2.7}$$

Electrical conductivity $\tilde{\sigma}$ characterizes free charge movement (creating electric current) when an electric field is present. Resistance to charge flow leads to energy dissipation. Dielectric permittivity $\tilde{\varepsilon}$ characterizes displacement of charge constrained in a material structure to the presence of an electric field. Charge displacement results in energy storage in the material. Magnetic permeability $\tilde{\mu}$ describes how intrinsic atomic and molecular magnetic moments respond to a magnetic field. For simple materials, distorting intrinsic magnetic moments store energy in the material [15].

For GPR, the dielectric permittivity is an important quantity. Most often, the terms relative permittivity or "dielectric constant" are used and defined as follows [15].

$$\kappa = \frac{\varepsilon}{\varepsilon_0} \tag{2.8}$$

Where ε_0 is the permittivity of vacuum, 8.89×10^{-12} F/m

2.3.4 Material properties

Ground penetrating radar is most useful in low-electrical-loss materials. If $\sigma = 0$, GPR would see very broad use since signals would penetrate to great depth. In practice, low-electrical-loss conditions are not prevalent. Clay-rich environments or areas of saline groundwater can create conditions where GPR signal penetration is very limited [15].

Earth materials are invariably composites of many other materials or components. Water and ice represent the few cases where a single component is primarily present. A simple beach sand is a mixture of soil grains, air, water, and ions dissolved in water. Soil grains will typically occupy 60-80% of the available volume. Understanding the physical properties of mixtures is thus a key factor in the interpretation of a GPR response [15].

Signal attenuation is primarily influenced by effective electrical conductivity and sometimes expressed in terms of the loss tangent, which increases with frequency, moisture content and the presence of dissolved salts. This will basically influence the

depth of penetration of the signal and hence useful range of the radar system, which is inversely related to this property. Greatest penetration is possible when the concrete is dry and the frequency low. However, the ability to resolve a small target improves as signal frequency and bandwidth increase and so antenna selection is a compromise between requirements for depth of penetration and resolution of detail [20].

Table 2. 1: Approximate relationship of pulse duration, frequency, depth and resolution [16].

Target depth*,m	Pulse duration†,ns	Centre frequency‡	Depth resolution§,m
< 0.25	0.5	2 GHz	0.03
< 0.5	1	1 GHz	0.05
< 1.0	2	500 MHz	0.1
< 2.0	4	250 MHz	0.2
< 4.0	8	125 MHz	0.4
< 8.0	16	63 MHz	0.8
< 16.0	32	31 MHz	1.6

*Depth in a medium loss(<20 dBm^{-1} attenuation) material
†Pulse duration to the half-power width of the main peak
‡Assumes a transmitted pulse in the general form of a Rayleigh wavelet
§Assumes a material of relative permittivity equal to 9

2.3.5 Velocity of propagation

In free space the velocity of propagation of electromagnetic waves is taken as 3×10^8 ms^{-1} however, in a dielectric this velocity will be reduced. If the propagation velocity in a material can be measured, or derived, an absolute measurement of the depth of a target or the thickness of the material can be made. For homogeneous, isotropic materials, the propagation velocity,v, can be calculated from equation 2.9, [16].

$$v = \frac{c}{\sqrt{\varepsilon_r}} \tag{2.9}$$

where c is the velocity of propagation in free space and ε_r, is the relative dielectric constant, or relative permittivity, of the material. The depth to a target can then be derived from equation 2.10,

$$d = v\,\frac{t_r}{2} \quad \text{(metres)} \tag{2.10}$$

Where t_r is the is the round-trip transit time to and from the target.

2.3.6 Target scattering

In general, ground penetrating radar enables any dielectric discontinuity to be detected and this includes nonmetallic as well as metallic targets. Targets can be classified according to their geometry: planar interfaces; long, thin objects; localized spherical or cuboidal objects, etc. The radar system can be designed to detect a given target type and is potentially capable of producing an image of the target in three dimensions, although less work has been done on this aspect of image presentation. Most radar images are either produced as two-dimensional representations, using either horizontal (x) and depth (E) axes or a horizontal plane representation (x,y) at a given depth [16].

In free space the radar cross-sectional area of a target is defined by its geometry and area, aspect and polarization. For ground penetrating radar it is necessary to consider additional factors, namely the coefficients of reflection and transmission as the wave passes through the dielectric to the target [16].

In [16] the intrinsic impedance η of a medium is defined by equation 2.11 as the relationship between the electric field, E, and the magnetic field, H.

$$\eta = \frac{E}{H} \tag{2.11}$$

η is a complex quantity that is calculated according to equation 2.11,

$$\eta = \left(\frac{-j\omega\mu}{\sigma - j\omega\varepsilon}\right)^{1/2} \tag{2.12}$$

In a nonconducting medium σ = 0 and the intrinsic impedance of the medium becomes.

$$\eta = \left(\frac{\mu}{\varepsilon}\right)^{1/2} = \sqrt{\mu}\left[\varepsilon'\left(1 - j\frac{\varepsilon''}{\varepsilon'}\right)\right]^{-1/2} \tag{2.13}$$

At the boundary between two media, some energy will be reflected and the remainder transmitted. In [16] the reflected field strength is described by the reflection coefficient, Γ as follows,

$$\Gamma = \frac{\eta_1 - \eta_2}{\eta_1 + \eta_2} \tag{2.14}$$

where η_1 and η_2 are the impedances of medium 1 and medium 2.

In a nonconducting medium, such as dry soil or dry concrete, and when considering only a single frequency of radiation the above expression may be simplified and rewritten as equation 2.15, [16].

$$\Gamma = \frac{\sqrt{\varepsilon_{r_1}} - \sqrt{\varepsilon_{r_2}}}{\sqrt{\varepsilon_{r_1}} + \sqrt{\varepsilon_{r_2}}} \tag{2.15}$$

where ε_r, is the relative permittivity of the medium.

The reflection coefficient has a positive value when $\varepsilon_{r_1} > \varepsilon_{r_2}$ such as where an air-filled void exists in a dielectric material and negative when $\varepsilon_{r_1} < \varepsilon_{r_2}$ such as where a metal target is present. The effect on a pulse waveform is to change the phase of the reflected wavelet, so that targets with different relative permittivities to the host material show different phase patterns of the reflected signal; hence the composition of the target may be determined. The amplitude of the reflected signal is affected by the propagation dielectric of the host material and the geometric characteristics and dielectric parameters of the target [16].

2.4 Impulse GPR design parameters

Radars that acquire data in the time domain are generally known as impulse. A time domain pulse is transmitted and the reflected energy is received as a function of time [21].

Besides data processing and display, there are 4 distinguished parts of impulse GPR: the transmitter, antennas, receiver and timing circuit. See Figure 2.5 which shows the block diagram of impulse GPR.

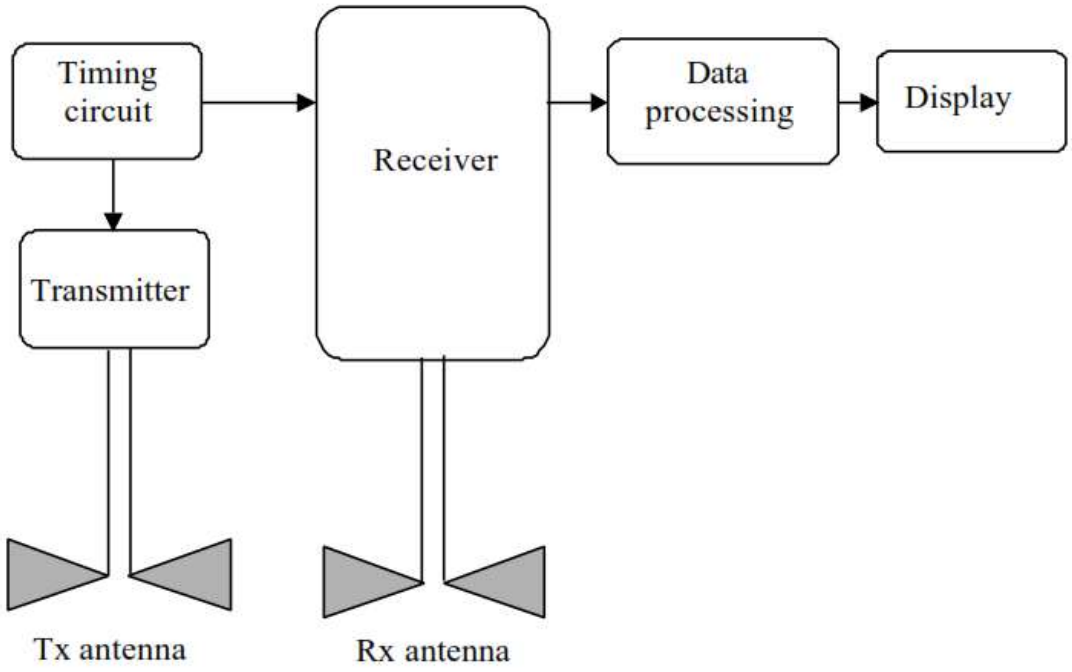

Figure 2. 5: Block diagram of a time domain GPR [22].

- **Transmitter**

The transmitter is a pulse generator, producing short transient pulses with a certain periodicity. This periodicity is called the pulse repetition frequency (PRF). The shape of the pulse is usually a monocycle or a Gaussian pulse, but other shapes like a

derivative of a Gaussian pulse or even a step are possible. The impulse generator is generally based on the technique of rapid discharge of stored energy in a capacitor or short transmission line [22].

A block diagram of the principle of pulse generation is shown in Figure 2.6.

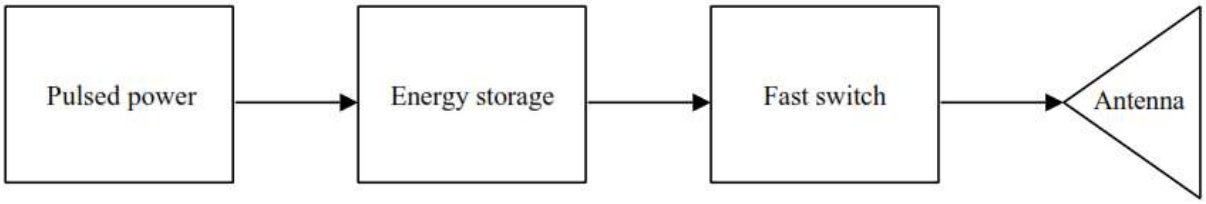

Figure 2. 6: Block diagram of pulse generator [22].

The fast switch is an important component in Figure 2.6 above. The most commonly used technologies for fast switches in GPR are semiconductor switches based on avalanche transistors, step-recovery diodes (SRD) or a combination of these two. In the latter, the SRD is then used to enhance the rise-time of the transition [22].

For the impulse radar choice of waveform and duration of the pulse is critical. The advantage of a monocycle in comparison with a monopulse is that the frequency spectrum of the first one decreases to zero at low frequencies, which cannot be efficiently transmitted via the antenna system, while the frequency spectrum of the second one has a global maximum there [23].

In [23] a pulse duration of 0.8ns is chosen (a period of approximating ideal monocycle). The frequency spectrum of such pulse covers interval from 210 MHz till 2100MHz on 10dB level. At frequencies below 1GHz, attenuation losses in the ground are small and considerable penetration depth can be achieved. However, landmine detection requires down-range resolution (in the ground) of the order of several centimeters, which can be achieved using frequencies above 1GHz. In [23] it was found experimentally that 0.8ns monocycle satisfies penetration and resolution requirements. The spectrum of this

pulse has a maximum at frequencies where the attenuation losses in the ground start to increase. So the spectral content of the monocycle below this maximum penetrates deep into the ground and the spectral content above this maximum provides sufficient down-range resolution.

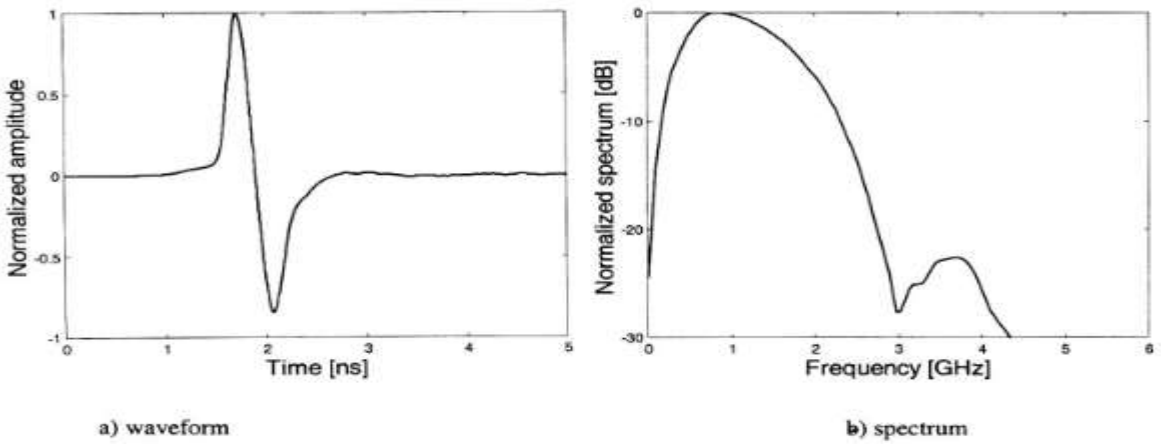

Figure 2. 7: Output signal from the 0.8ns generator [23].

- **Antennas**

Antennas are one of the most critical parts in ground penetrating radar (GPR) systems. They substantially determine the quality of the obtained GPR raw data. In the time domain, a narrow-band antenna produces strong multiple reflections at the antenna ends and feed point referred to as late-time ringing. For an application such as landmine detection, the late time ringing should be minimal to avoid masking of targets. Ultra-wideband antennas are therefore highly required by impulse GPR systems [1].

The majority of GPR systems have separate antennas for transmitting and receiving (bi-static operation), with some antennas having a fixed separation while others can be varied. Antenna separation should be as small as possible based on the needs of the survey and the wavelength of the antennas. The depth resolution of targets decreases as the distance between antennas increases, however this effect is not significant until the

antenna separation nears half of the target depth. A safe antenna separation, if there is very little site information available, is 20% of the target depth [24].

- **Receiver**

From the hardware point of view, the receiver is the most difficult block to build. Its performance has a direct impact on the over-all system performance. The receiver has to be very sensitive, posses a large fractional bandwidth, a large dynamic range and a good noise performance. Figure 2.8 shows the block diagram of the receiver. From the left to the right we have, Radio Frequency(RF) signal, a time-varying gain (TVG) amplifier, a low noise amplifier (LNA), a sample and hold circuit (S/H) and an analog-to-digital converter (A/D converter) [22].

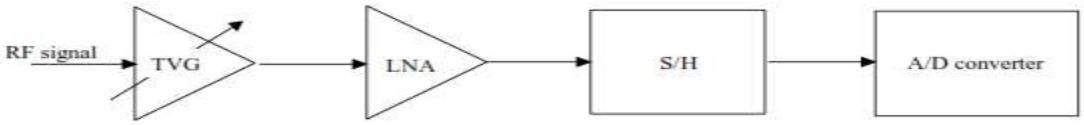

Figure 2. 8: Block diagram of receiver [22].

- **Timing circuit**

The receiver in a time domain GPR is based on a non-coherent acquisition of the backscattered RF signal. This means that the acquisition must be controlled by a very stable and precise timing circuit that synchronizes the work between the different parts in the system [22].

The timing circuit is responsible for mainly three things. First, it has to trigger the impulse generator. Secondly, the timing circuit has to generate the timing signals as needed for the sequential sampler, *i.e.* a trigger for the A/D converter at the intersection of the fast and the slow ramp. Third, it has to control the timing for the TVG [22].

2.5 Applications of GPR

GPR is a rapidly growing field that has seen tremendous progress in the development of theory, technique, technology, and range of applications over the past 15–20 years [21].

The range of applications for ground penetrating radar is considerable. Typical examples include the detection of buried, explosive, non-metallic mines, buried ordnance, caches of arms and explosives. Other possibilities include archaeological investigation, assessment of road construction, assessment of bridge structures, tunnel linings, geological formations and forensic investigation. With such a wide range of applications it is only possible to highlight selected applications [16].

GPR is one of a number of technologies that has been extensively researched as a means of improving the efficiency of mine clearance operations. There are two main areas of application, civil and military. Civilian or humanitarian landmine clearance is aimed at restoring land to the population and the goal is the complete removal of all landmines and unexploded ordnance (UXO). Military programmes are largely based on the requirement to maintain the pace of military operations and have different needs in terms of speed and detection performance to civil or humanitarian programmes [25].

GPR technology is capable of providing information on fractures, previous reconstructions, material integrity and a variety of the characteristics of building materials. For this reason, GPR has found a multitude of applications in studying the integrity of historical buildings. GPR surveying can effectively identify critical structural supports such as rebar and tension ties in walls that help to constrain the horizontal load forces. After earthquakes or landslides, the changes and hidden damage to structures can be detected using radar. In the case when GPR is used to monitor a building, recordings at time 1 and time 2 can be differenced to indicate only those areas which have undergone changes since the last survey [18].

CHAPTER III

Ultra-Wideband Antennas

3.1 General Concepts of Antennas

An antenna is defined by Webster's Dictionary as "a usually metallic device (as a rod or wire) for radiating or receiving radio waves." The *IEEE Standard Definitions of Terms for Antennas* (IEEE Std 145–1983) defines the antenna or aerial as "a means for radiating or receiving radio waves." In other words the antenna is the transitional structure between free-space and a guiding device, as shown in Figure 3.1. The guiding device or transmission line may take the form of a coaxial line or a hollow pipe (waveguide), and it is used to transport electromagnetic energy from the transmitting source to the antenna, or from the antenna to the receiver. In the former case, we have a transmitting antenna and in the latter a receiving antenna [26].

Antennas act as the transition between space and circuitry. They convert photons to electrons or vice versa. A photon is a quantum unit of electromagnetic energy equal to hf, where h = Planck's constant ($= 6.63 \times 10^{-34}$ Js) and f = frequency (Hz) [27].

Regardless of antenna type, all involve the same basic principle that radiation is produced by accelerated (or decelerated) charge. The basic equations of radiation may be expressed simply as follows by equation 3.1, [27].

$$iL = Q\dot{v} \text{ (A m } s^{-1}\text{) Basic radiation equation} \quad (3.1)$$

where i = time-changing current, A s^{-1}

L = length of current element, m

Q = charge,C

$\dot{v}$ = time change of velocity which equals the acceleration of the charge, m s^{-1}

Thus, time-changing current radiates and accelerated charge radiates. The radiation is perpendicular to the acceleration, and the radiated power is proportional to the square of iL = $Q\dot{v}$ [27].

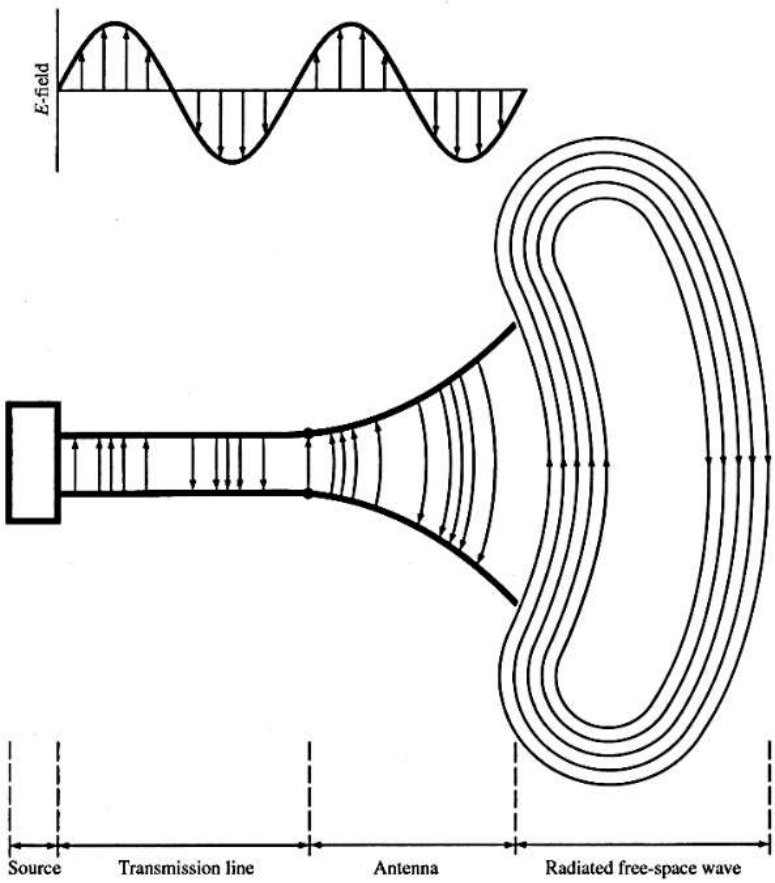

Figure 3. 1: Antenna as a transition device [26].

3.2 Dipole and Bow-tie antenna

A dipole is the simplest antenna that is still frequently used for GPR mainly because of its simplicity. The main drawback of a dipole for GPR application is its inherent narrowband nature. In most of ultra-wideband applications this drawback is dealt with by means of resistive loading, which can improve the dipole's bandwidth considerably by suppressing reflections from the dipole ends. Application of resistive loading is however a tradeoff for bandwidth improvement which is achieved at the expense of a significant reduction in radiation efficiency [19].

A bow-tie UWB antenna is widely used in the design for GPR applications, as it has the ability to reduce ground susceptibility during GPR operations [28], [29].

Figure 3.2 shows a simple bow-tie antenna design which consists of two flares connected to a common feed.

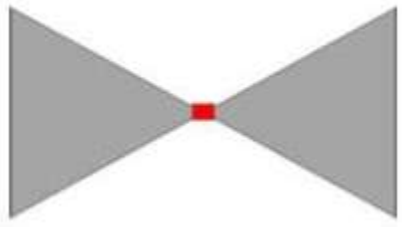

Figure 3. 2: Bow-tie antenna design [29].

The planar structure of bow-tie antennas is especially attractive for use in a compact GPR system like many commercially available systems. However, because of their open structure in most cases bow-tie antennas are equipped with a shielding box to minimize electromagnetic interference (EMI). Such a shielding box should be designed properly in order not to degrade the antenna performance [19].

3.3 Ultra-Wideband Antennas

It should come as no surprise that large bandwidth is what distinguishes a UWB antenna from antennas in general. There are two criteria available for identifying when an antenna may be considered ultra-wideband. In 1990, a Defense Advanced Research Projects Agency(DARPA) report required a UWB radar to have a fractional bandwidth greater than 0.25. An alternate and more recent definition, due to the United States Federal Communications Commission (FCC), places the limit at 0.20 [30].

In [30] fractional bandwidth, b_w is given by equation 3.2,

$$b_w = 2\frac{f_H - f_L}{f_H + f_L} \geq \begin{cases} 0.25 & \text{DARPA} \\ 0.20 & \text{FCC} \end{cases} \tag{3.2}$$

Where f_H is the upper, or high, end of the antenna's operational band and f_L is the bottom, or low, end of the antenna's operational band. Additionally, the FCC provides an alternate definition whereby a UWB antenna is any antenna with a bandwidth greater than 500 MHz.

According to the FCC, the upper and lower ends of the operational band are defined by the points where the radiated power is down 10 dB from its peak level. This FCC definition does not, strictly speaking, define antenna bandwidth because the radiated power also depends on the spectral response of the transmitted power. In addition, the FCC and DARPA definitions of fractional bandwidth in (3.2) are really only for regulatory purposes. The relation of (3.2) assumes the center frequency is the arithmetic average of the upper and lower operating frequencies. For a variety of reasons, the geometric average should be used instead. In addition, a 500 MHz bandwidth at 10 GHz is only a 5% fractional bandwidth, yet would be considered UWB for regulatory purposes [30].

The imminent widespread commercial deployment of ultra-wideband (UWB) systems has sparked renewed interest in the subject of ultra-wideband antennas. The

power levels authorized by the FCC mean that every dB counts in a UWB system - as much as or perhaps even more so than in a standard narrowband system. Thus, an effective UWB antenna is a critical part of an overall UWB system design [31].

3.4 Dispersion and UWB Antennas

Dispersion is a problem for multi-band systems as well as those where a radiated signal occupies the entire band. If an antenna behaves differently at different look angles or at different frequencies, then a UWB system must compensate for these differences. This compensation may be difficult and resource intensive. Further, there is no guarantee that the performance of a dispersive antenna may be made equivalent to that of a non-dispersive antenna [32].

Classical frequency independent antennas (a type of UWB antenna) rely on variations in geometry to obtain their broadband behavior. A smaller scale portion radiates high frequency components and a larger scale portion radiates lower frequency components of a signal. Because the phase center moves as a function of frequency, frequency independent antennas radiate dispersed signals [32].

For instance, consider a log spiral antenna. Figure 3.3 shows a 1-11 GHz log spiral antenna. This antenna is fed from the tip of the cone where the spiral has a smaller scale. Lower frequency components must propagate to the larger scale structure at the base of the antenna before they radiate. Figure 3.4 shows the result of this physical structure on a received signal. The transmit antenna accepts a transmitted impulse voltage signal (left/red) at its terminals. A receive antenna then yields a received impulse voltage signal (right/blue) at its terminals. The dispersion of the log spiral antennas used for both transmit and receive results in a dispersed receive signal. This dispersion is clearly manifest in two respects. First, the received signal has a temporal extent over twice as long as the transmit signal. Second, the received signal shows a distinct "chirp." The

earlier portion of this signal exhibits relatively high frequency content with a shorter time duration between zero crossings. The later portion of the received signal exhibits relatively low frequency content with a longer time duration between zero crossings [32].

Figure 3. 3: Log conical spiral antennas (©2004 H. Schantz) [32].

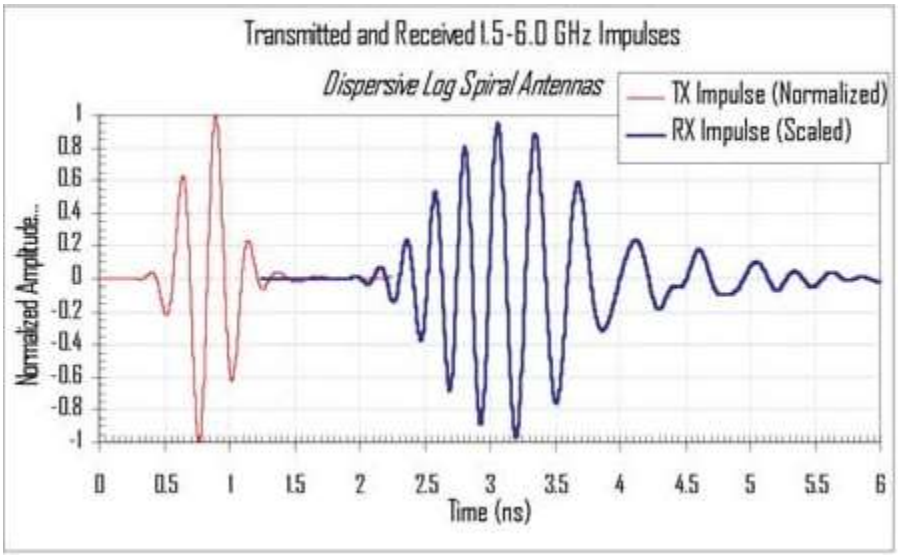

Figure 3. 4: Transmitted (left/red) and received (right/blue) voltage waveforms from a pair of conical log spiral antennas (©2004 H. Schantz) [32].

CHAPTER IV

Transverse Electromagnetic Horn Antenna

4.1 Introduction

Transverse Electromagnetic (TEM) horn antenna as the name suggests is an antenna that radiates TEM waves. The basic structure consists of two linear or exponential tapered metal plates that are guided by a parallel two-wire transmission line. As the TEM horn antennas form the transition of a parallel two-wire transmission line to the free space, such structures can be considered as the extension of a parallel two-wire transmission line [9].

TEM wave is a plane wave in space where the electric and magnetic field lines, E and H,are everywhere perpendicular to each other and perpendicular to the wave direction,as shown in Figure 4.1.E and H are also in phase and the wave equation is given by equation 4.1 [27].

$$\frac{\partial^2 E_y}{\partial t^2} = \frac{1}{\mu\varepsilon}\frac{\partial^2 E_y}{\partial x^2} \tag{4.1}$$

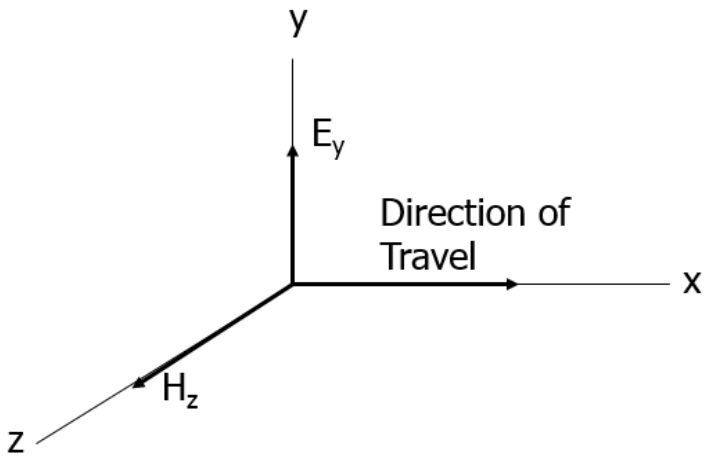

Figure 4. 1: TEM wave propagating in the x direction with E in the y direction (E_y) and H in the z direction (H_z).

The ratio of E_y to H_z is an impedance Z_0 as given by equation 4.2, [27].

$$Z_0(\Omega) = \frac{E_y}{H_z} = \sqrt{\frac{\mu}{\varepsilon}} \tag{4.2}$$

In [27] for air or vacuum $Z_0(\Omega)$ is given by equation 4.3.

$$Z_0(\Omega) = \frac{E_y}{H_z} = \sqrt{\frac{\mu}{\varepsilon}} = 377(\text{Intrinsic impedance of space}) \tag{4.3}$$

The transverse electromagnetic (TEM) horn antenna is a popular broadband antenna. The basic antenna is a simple design, consisting only of two triangular metal plates and a feeding structure. Neglecting the feeding structure for the moment, the horn is described completely by only three variables: α, β, and S [33].

As shown in Figure 4.2 and 4.3, it consists of two perfectly conducting triangular plates. The angle of each plate at the drive point of the horn is α ($0 < \alpha < 180^{\circ}$), and the angular separation between the plates is β ($0 < \beta \leq 180^{\circ}$) [33].

For special case $\beta = 180^{\circ}$,the plates are coplanar, and the geometry becomes that of the bow-tie antenna. A key parameter for the design of the horn is the characteristic impedance Z_c for the TEM spherical wave ($E_r = H_r = 0$) on the infinitely long antenna ($S \rightarrow \infty$) [33].

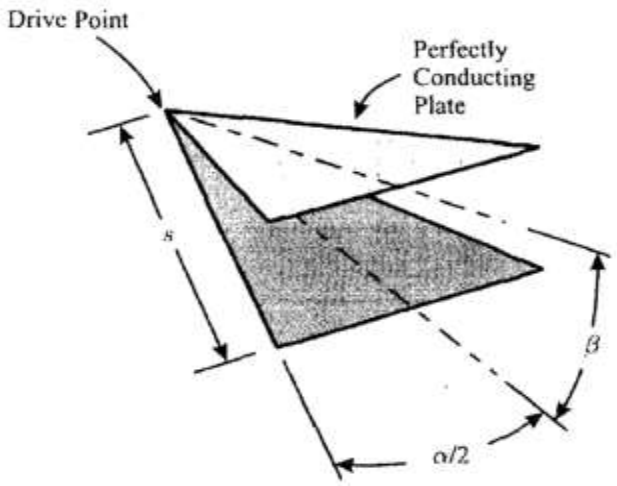

Figure 4. 2: The geometry for the basic TEM horn antenna [34].

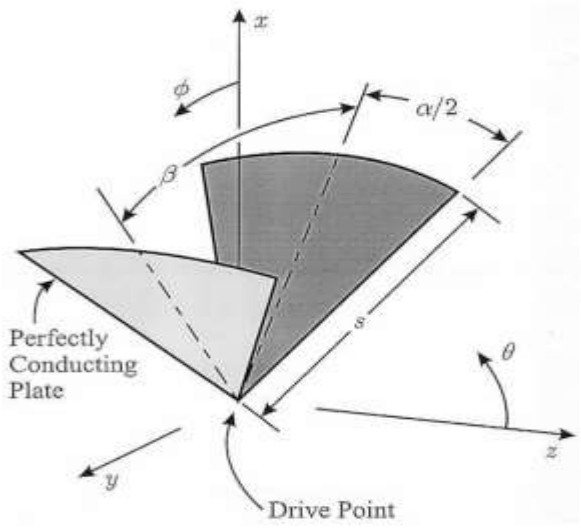

Figure 4. 3: Geometry for the TEM horn antenna [33].

4.2 Characteristic Impedance

In the limit as the antenna becomes infinitely long ($S \rightarrow \infty$), a characteristic impedance, Z_c, can be defined for the antenna. This is the impedance of the TEM transmission-line mode on the infinite structure. The characteristic impedance is a function of only the angles α and β [34].

Figure 4.4 is a graph of the relationship between these angles and the characteristic impedance.

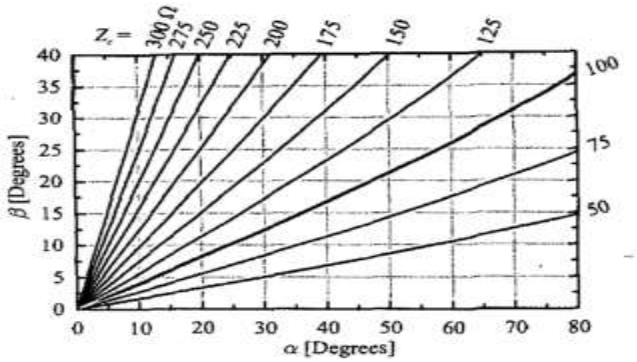

Figure 4. 4: The characteristic impedance, of the TEM horn antenna as a function of the angles α and β [34].

For an antenna of finite length that is reasonably long, the characteristic impedance of the antenna is a good approximation to the input impedance of the antenna. As an example, the calculated input impedance of an antenna with $\alpha = 47.30^o$ and $\beta = 20^o$ for which $Z_c = 100\Omega$,is shown as a function of the electrical length,s/λ,in Figure 4.5. The input resistance,R, oscillates around, 100 Ω and the reactance, X, oscillates around 0Ω . For antennas with $s/\lambda > 3$, the amplitude of the oscillations is fairly small,$\approx \pm 10\Omega$. To minimize the reflection at the transmission-line/antenna junction, the characteristic impedances of the feeding transmission line and the antenna are generally chosen to be the same value. With Z_c specified, one of the angles for the horn can be treated as a free variable and the other determined using Figure 4.4 [34].

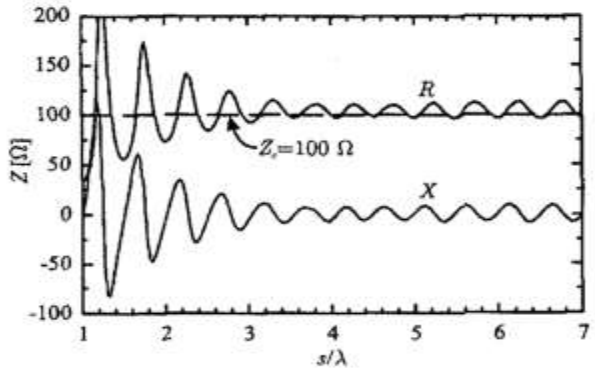

Figure 4. 5: The input impedance, Z = R + jX, versus electrical length of the horn antenna [34].

For the antenna in Figure 4.5, $\alpha = 47.30^{o}$, $\beta = 20^{o}$, and $Z_c = 100\Omega$

4.3 Input Impedance

Input impedance is defined as "the impedance presented by an antenna at its terminals or the ratio of the voltage to current at a pair of terminals or the ratio of the appropriate components of the electric to magnetic fields at a point." In Figure 4.6 these terminals are designated as a – b. The ratio of the voltage to current at these terminals, with no load attached, defines the impedance of the antenna [26].

$$Z_A = R_A + j X_A \tag{4.4}$$

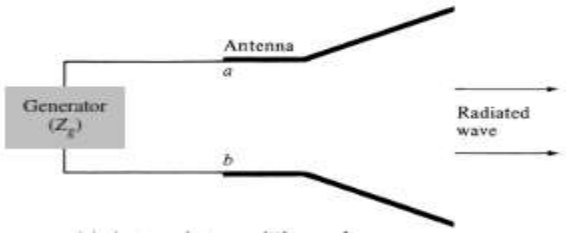

Figure 4. 6: Input impedance of a transmitting antenna [26].

Where,

Z_A = antenna impedance at terminals a – b (Ohms)

R_A = antenna resistance at terminals a – b (Ohms)

X_A = antenna reactance at terminals a – b (Ohms)

4.4 Basic wave types and principle of TEM mode generation

4.4.1 Basic wave types

There are four types of basic wave types as described below [35].

I. Transverse Electromagnetic Waves (TEM Waves). These waves contain neither an electric nor a magnetic field component in the direction of propagation. There is no E_z or H_z if e_z is the direction of propagation.

II. Transverse Magnetic Waves (TM or E waves). These waves contain an electric field component but not a magnetic field component in the direction of propagation. There is no H_z if e_z is the direction of propagation, that is, $\Psi(r) = 0$.

III. Transverse Electric Waves (TE or H waves). These waves contain a magnetic field component but not an electric field component in the direction of propagation. There is no E_z if e_z is the direction of propagation, that is, $\Phi(r) = 0$.

IV. Hybrid waves (HE or EH waves). These waves contain all components of electric and magnetic fields. These hybrid waves are obtained by linear superposition of TE and TM waves, that is, $\Psi(r) \neq 0$ and $\Phi(r) \neq 0$.

4.4.2 Principle of TEM mode generation

The basic structure of a TEM horn is composed of either two linearly or exponentially tapered plates. Unlike other general horn antennas, the two plates are separated and fed by a coaxial line [10].

TEM horn antenna is an Ultra-Wideband horn antenna without sidewalls, so it supports the TEM mode [36].

Theoretically a TEM mode does not have an upper cut-off frequency, in practice however this upper cut-off frequency will be limited. The dimension of the antenna mainly governs the lower cut-off frequency [37].

A travelling wave TEM horn consists of a pair of triangular conductors forming a V structure capable of radiating and receiving a fast transient pulse [38].

TEM horn, unlike a dipole antenna is an aperture type of antenna. This means the radiated field from the aperture of a TEM horn is a time derivative of the aperture field [39].

On transmission, the TEM horn radiates a signal that is proportional to the first time derivative of the incident voltage pulse in the feeding point. On reception, the horn outputs a voltage pulse that has the same shape as the incoming electric field [22].

TEM horn antenna is composed of two tapered metal plates, the current flows on these two plates and the TEM wave propagates between these two plates simultaneously. The current flowing on the two plates leads to the generation of the magnetic fields of TEM mode wave. The voltage difference between two plates leads to the generation of the electric fields of TEM mode wave [14]. See Figure 4.7 which shows TEM mode generation.

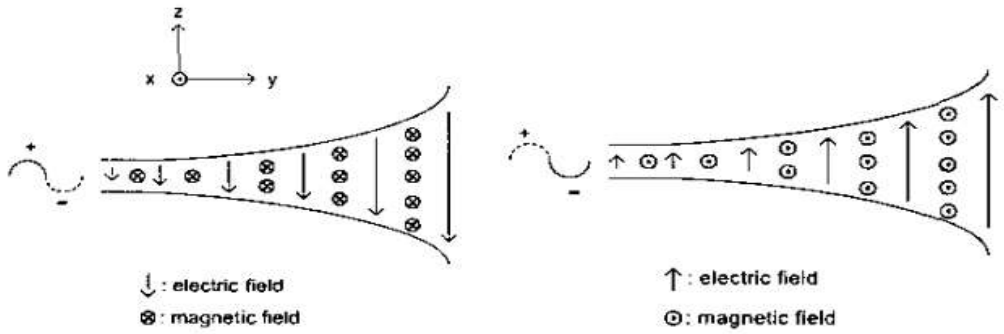

(a) When positive voltage is applied (b) When minus voltage is applied

Figure 4. 7: Principle of TEM mode generation [10].

Because of the presence of loss in resistively loaded TEM-horn plates, the field patterns for EM waves propagating between lossy plates deviate from a pure TEM mode thus a resistively loaded "TEM" horn cannot support a pure TEM mode [6].

4.5 How to supply Radio Frequency power to TEM horn antenna ?

TEM horns receive the RF power directly via coaxial connectors. Due to unbalance nature of a coaxial cable, the direct connection introduces two different currents (unbalance currents) on the plates of the TEM horn that is a balance antenna. This results in an unpredictable skew radiation pattern together with the degradation of the VSWR. A tapered balun is employed in so as to mitigate such deleterious effects. Such a balun has the advantages of being wideband and mechanically suitable for connecting to TEM horns [40].

A coaxial cable should not directly be connected to the input of a TEM horn because of two reasons. Firstly, a coaxial cable is an unbalance transmission line, whereas the TEM horn is a balance antenna. Consequently, the direct connection introduces two different currents (unbalance currents) on the plates of the antenna and also induces the currents upon the outside of the cable, resulting in an unpredictable skew radiation pattern

together with the degradation of the VSWR. Secondly, since there is usually a mismatch between the coaxial cable impedance and the input impedance of the antenna, a part of the transmitted signal is reflected from the junction, increasing the VSWR. In order to mitigate these deleterious effects, a balun (balance to unbalance transformer) is put between the coaxial cable and the balance antenna. A balun is built by slicing the outer conductor of a coaxial line diagonally over its length [13].

In [7] a TEM horn is fed via a 50 Ω coaxial line without balun but Unbalanced feeding of the antenna did not cause any problems except for a common-mode current, reflected from the antenna and propagated outside the coaxial line. This current was absorbed by a soft absorbing material applied around the coaxial line.

4.6 Tapering

To achieve good performance, impedance variation between feed point and aperture of the TEM horn antenna should be continuous and smooth [41].

Linear tapered antennas can be built easily as compared to an exponentially tapered antenna. However, exponentially tapered plates have the advantage of smooth impedance variations [42].

For a TEM horn with a linearly tapered shape, a resistively loaded taper is used to reduce reflections [43].

To achieve good impedance matching without resistive loading, typical tapered transmission lines are applied to the antenna shape, i.e., the separation of two plates [43].

4.6.1 Types of tapering

Common taper shapes are exponential, triangular, Klopfenstein, Hecken and Chebyshev types. Each antenna exhibits a satisfactory reflection characteristic over the broadband frequency range owing to the effects of impedance matching by the tapered transmission lines [43].

The antennas applying the triangular and Klopfenstein tapers have many large ripples in the gain profile [43]. The antenna with the exponential taper has flat gain characteristics (meaning a regular and constant gain), allowing it to be used as a broadband antenna [43].

A Chebyshev tapered structure improves directivity of the antenna, and yields the smallest minor-lobe amplitude for a fixed taper length [12].

4.6.2 How to physically taper the characteristics impedance ?

Most tapered lines are implemented in stripline or microstrip. As a result, we can modify the characteristic impedance of the transmission line by simply tapering the width W(z) of the conductor. In other words, we can continuously increase or decrease the width of the microstrip or stripline to create the desired impedance taper Z(z).The bandwidth of a multi-section matching transformer increases with the number of sections. Similarly, the bandwidth of a tapered line will typically increase as the length L is increased [44].

4.7 Merits of TEM Horn Antenna

A TEM horn antenna provides minimum-duration response to impulsive input or output fields and is able to discriminate between events occurring in the time domain. This is done by limiting the amount of propagation moding in the antenna and by having a good impedance match design both at the feed-point to the antenna and at the aperture of the antenna. Inside the antenna, the fields should remain in the dominant mode, which for our antenna is the TEM mode. In other antennas, such as the log-periodic antenna, the spiral antenna, or the pyramidal horn antenna, phase dispersion occurs as the wave propagates along each of the elements, resulting in a greatly extended antenna response time to the fields [4].

This is shown in the time-domain plot of Figures 4.8 and 4.9. Figure 4.8 shows the impulse response of the TEM horn antenna to the input waveform of an impulse generator for a waveform having a pulse width of approximately 300 ps. The TEM horn response time is on the order of a few nanoseconds. We can see that the TEM-horn antenna can accurately reproduce the incoming response of the surrounding environment and can resolve scattering events on the order of approximately 5 ns. The impulse response of a log-periodic antenna is shown in Figure 4.9, and is on the order of 40 ns. In this case, if we were trying to localize two events that are 10 ns apart, say reflections from the walls of a chamber, then the TEM horn antenna can discriminate between these events, but the log-periodic antenna cannot [4].

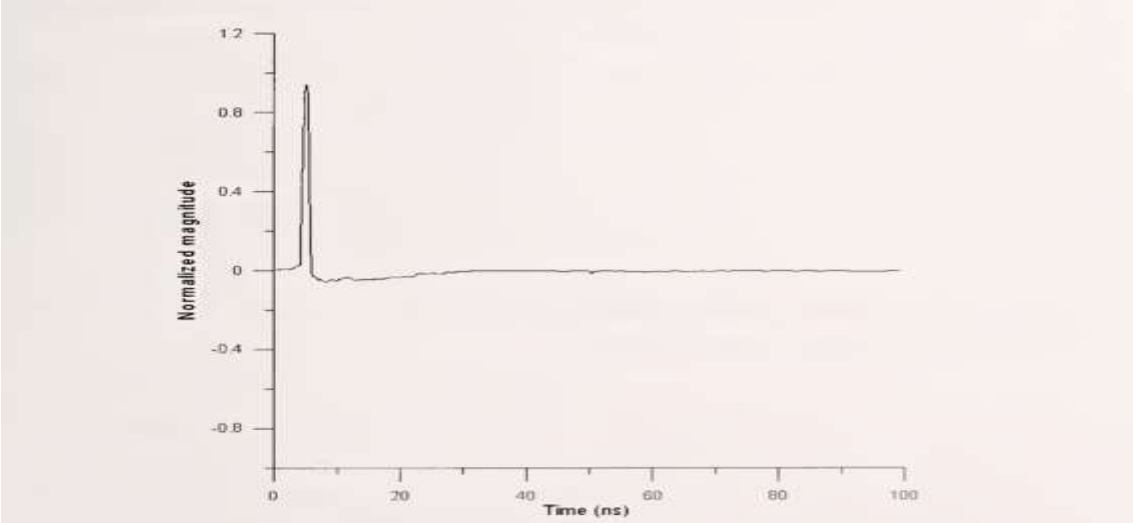

Figure 4. 8: Time-domain response of TEM horn antenna to an applied impulsive electric field [4].

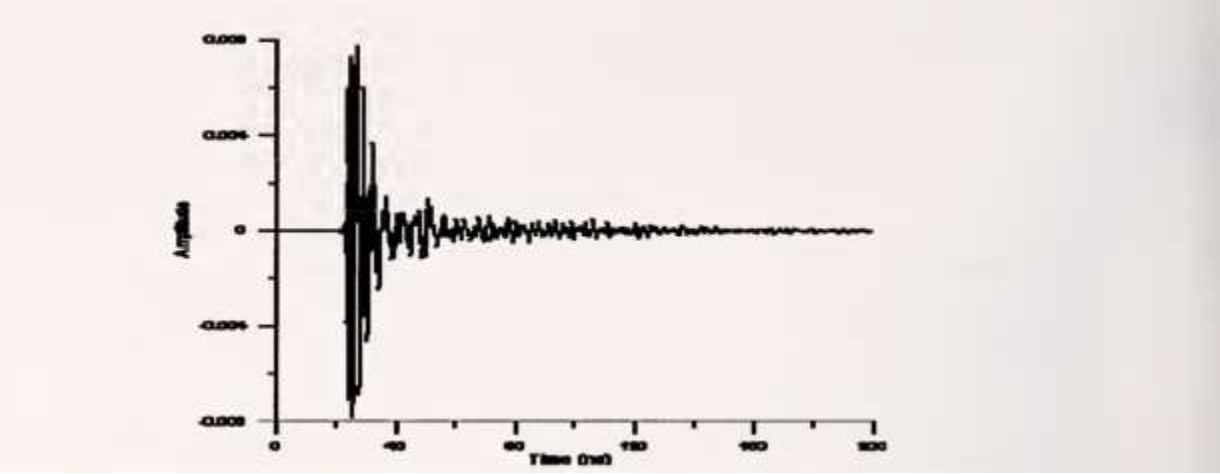

Figure 4. 9: Time-domain response of log-periodic antenna to an impulsive electric field [4].

The linear phase response of a TEM horn occurs because the antenna elements maintain the proper field and current relationships, by means of correct width and height ratios [4].

The design of most electromagnetic compatibility (EMC) antennas results in a nonlinear antenna phase response as a function of frequency. The time-domain signature for an log-periodic dipole antennas (LPDA) is shown in Figure 4.10. The response duration of the antenna is on the order of 100 ns. This extended temporal response makes it difficult to separate scattering events. For example, suppose we want to look at either the antenna response or the ground bounce. Ground bounce will typically follow the direct coupling between antennas by a few nanoseconds. Thus, the long ring-down times of the LPDA do not allow us to easily resolve the ground bounce effects. On the other hand, the TEM-horn antenna has a very short impulse response. This response is shown in Figure 4.11 and is approximately 5 ns in duration. Thus, the TEM-horn antenna accurately reproduces the incoming response of the surrounding environment and resolves scattering events. Figure 4.12 shows the time domain response of the 0.36 m TEM-horn antenna in the presence of ground bounce. Notice that both events can be separated in time and studied individually using signal processing techniques [45].

TEM horn antenna is an important ultra-wideband antenna. It has a fixed phase center and a strong ability of directional radiation, which is an ideal form of transient antenna [46].

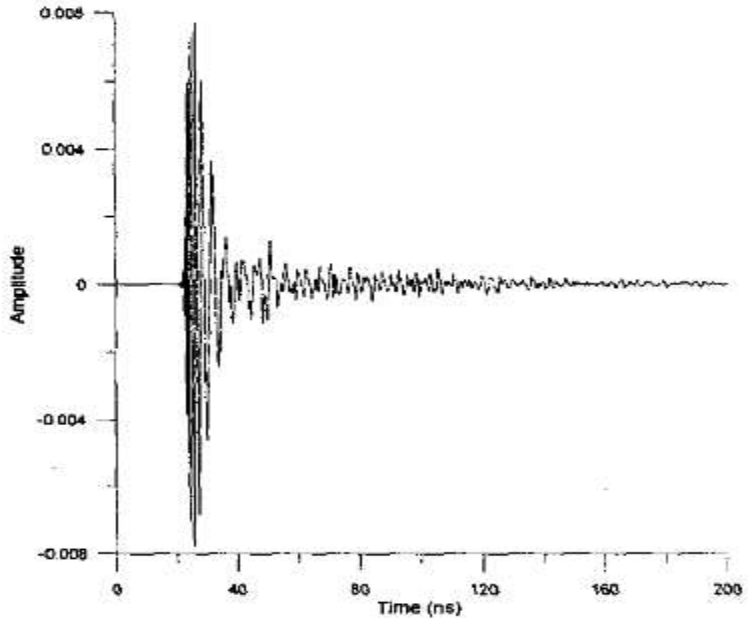

Figure 4. 10: Impulse response of log-periodic antenna [45].

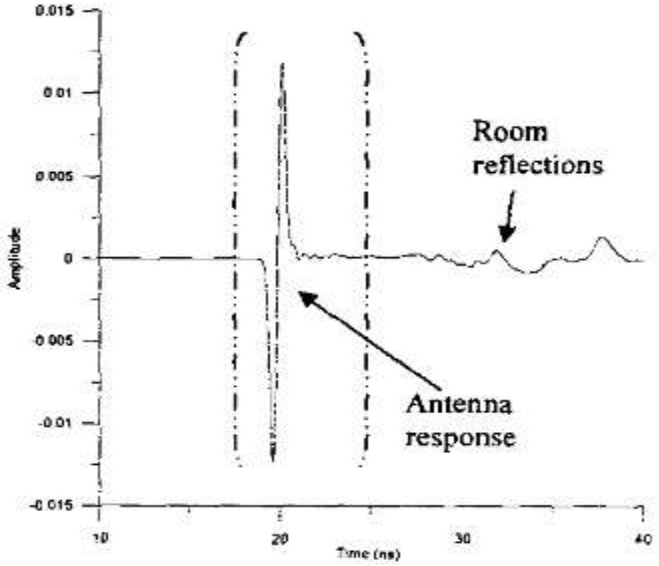

Figure 4. 11: Impulse response of 1.2 m TEM-horn antenna shown by the dashed parentheses [45].

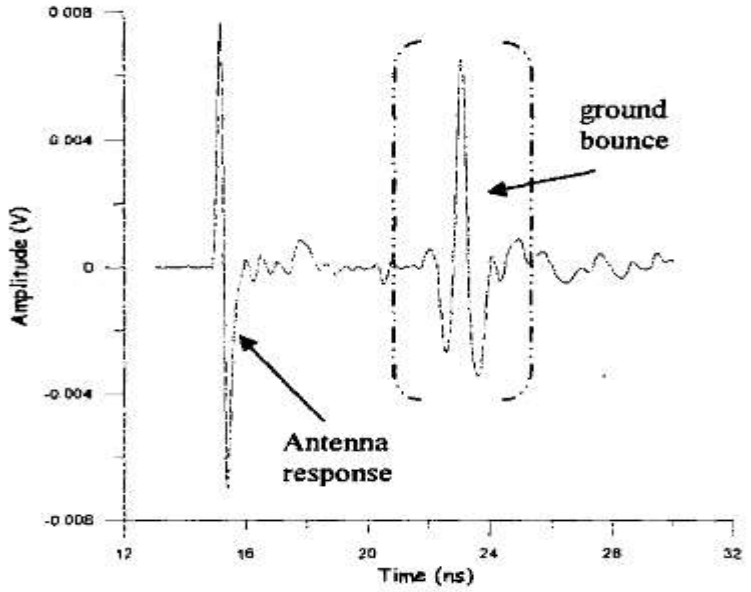

Figure 4. 12: Impulse response of 0.36 m TEM-horn antenna in presence of ground bounce (dashed brackets) [45].

CHAPTER V

Design of Improved TEM Horn Antenna

5.1 Improved TEM horn antenna design using double exponential approach

TEM120cm with 200,250 and 377 Ohm aperture impedance and TEM60cm with 200,250 and 377 Ohm aperture impedance are designed and simulated using double exponential approach as described below.

Double exponential approach is an approach where both the characteristics impedance variation along the TEM horn antenna and the separation distance between the upper and lower conductors of the TEM horn antenna are described by exponential equations as explained below.

The characteristics impedance of the antenna is set in accordance with the following exponential equation 5.1,

$$Z(x) = Z_0 e^{cx},\ c = \frac{\ln(Z_{ap}/Z_0)}{L} \tag{5.1}$$

Where,

$Z(x)$ is the characteristics impedance of the TEM horn as a function of x.

x is the length of the TEM horn along the X-axis, $0 \leq x \leq L$.

Z_0 is the impedance of the feed line(50 Ω).

Z_{ap} is the chosen aperture impedance of the TEM horn(200,250 and 377 Ω are chosen).

L is the length of the TEM horn (In this thesis work L is chosen as 60 and 120 cm).

Separation between the upper and lower conductors of the TEM horn is also chosen to be an exponential function of the distance as given by equation 5.2,

$$d(x) = d_0\ e^{bx},\ b = \frac{\ln(d_L/d_0)}{L} \tag{5.2}$$

Where,

d(x) is the separation between the upper and lower conductors of the TEM horn as a function of x .

x is the length of the TEM horn along the X-axis, 0≤ x ≤ L.

d_0 is the spacing at the feed and in this thesis work it is chosen to be 2 mm= 0.2 cm .

d_L is the spacing at the mouth of the TEM horn and is dependent on the minimum cut off frequency of the TEM horn.

L is the length of the TEM horn (L is chosen as 60 and 120 cm).

The width of the TEM horn is given by equation 5.3,

$$w(x) = Z_{ap} * \frac{d(x)}{Z(x)} \tag{5.3}$$

Where,

$w(x)$ is the width of the TEM horn as a function of $\boldsymbol{x}$.

Z_{ap} is the chosen aperture impedance of the TEM horn(200,250 and 377 Ω are chosen).

$d(x)$ is the separation between the upper and lower conductors of the TEM horn as a function of x given by equation (5.2).

$Z(x)$ is the characteristics impedance of the TEM horn as a function of $\boldsymbol{x}$ given by equation (5.1).

Generally, TEM horn antennas act as high pass filters with cut off frequency determined from the conductor plate length. For a given frequency range, the lowest frequency component when no resistive loading is used, determines the antenna length. In multiple quarter wavelength transformer (transmission line theory), it is a common practice to match the "input" to "load" impedance by using line length at least one wavelength, $\boldsymbol{1\,\lambda}$ [9].

The conductor plate spacing at the "mouth" should be at least half wavelength ($\boldsymbol{\lambda/2}$) long [9].

Six TEM horn antennas are designed and simulated in FEKO. See table 5.1 and 5.2 for the summary of dimensions and design equations of each TEM horn antenna respectively.

Table 5. 1: Summary of designed TEM horn antenna dimensions

Item #	Antenna length (cm)	Feed line impedance (Ohm)	Aperture impedance (Ohm)	Spacing at feed (cm)	Spacing at aperture (cm)	Width at feed (cm)	Width at aperture (cm)
1	120	50	200	0.2	60	0.8	60
2	120	50	250	0.2	60	1	60
3	120	50	377	0.2	60	1.508	60
4	60	50	200	0.2	30	0.8	30
5	60	50	250	0.2	30	1	30
6	60	50	377	0.2	30	1.508	30

Table 5. 2: Summary of TEM horn antenna design equations

Item #	Antenna length (cm)	Feed line impedance (Ohm)	Aperture impedan-ce (Ohm)	Impedance ,Z(x) (Ohm)	Spacing, d(x) (cm)	Width, w(x) (cm)
1	120	50	200	$\mathbf{50e^{0.01155x}}$	$\mathbf{0.2e^{0.04753x}}$	$\mathbf{0.8e^{0.03598x}}$
2	120	50	250	$\mathbf{50e^{0.0134x}}$	$\mathbf{0.2e^{0.04753x}}$	$\mathbf{e^{0.03412x}}$
3	120	50	377	$\mathbf{50e^{0.016835x}}$	$\mathbf{0.2e^{0.04753x}}$	$\mathbf{1.508e^{0.0307x}}$
4	60	50	200	$\mathbf{50e^{0.0231x}}$	$\mathbf{0.2e^{0.0835x}}$	$\mathbf{0.8e^{0.0604x}}$
5	60	50	250	$\mathbf{50e^{0.0268x}}$	$\mathbf{0.2\ e^{0.0835x}}$	$\mathbf{e^{0.0567x}}$
6	60	50	377	$\mathbf{50e^{0.03367x}}$	$\mathbf{0.2e^{0.0835x}}$	$\mathbf{1.508e^{0.04983x}}$

The detail design and simulation work of TEM120cm with 200 Ohm aperture impedance is elaborated in Appendix C and in sections 5.2 to 5.7.

5.2 TEM120cm with 200 Ohm aperture impedance design

The designed new antenna should operate for at least a decade with lowest frequency at **250 MHz.**

- The TEM horn antenna length should be not less than 1 $\boldsymbol{\lambda}$
- Therefore, $\lambda = 300/250 = 1.2$ m or 120 cm
- Substituting Z_0 as 50 Ω, Z_{ap} as 200 Ω and L as 120cm in equation (5.1) we get the characteristics impedance of the TEM horn is given as

$$Z(x) = 50\, e^{0.01155\ x} \quad (cm) \tag{5.4}$$

- Substituting d_0 as 0.2 cm, $d_L = \lambda/2 = 60$ cm and L as 120cm in equation (5.2) we get the separation between the upper and lower conductors of the TEM horn as a function of x as

$$d(x) = 0.2\, e^{0.04753\ x} \quad (cm) \tag{5.5}$$

- Substituting Z_{ap} as 200 Ω, $d(x) = 0.2\, e^{0.04753\ x}$ and $Z(x) = 50\, e^{0.01155\ x}$ in equation (5.3) we get the width of the TEM horn as a function of x as

$$w(x) = 0.8 * e^{0.03598\ x}\ (cm) \tag{5.6}$$

The TEM horn is simulated in FEKO and the 3D view of the simulated TEM horn is shown in Figure 5.1. The detail step of the design work in FEKO is found in Appendix C.

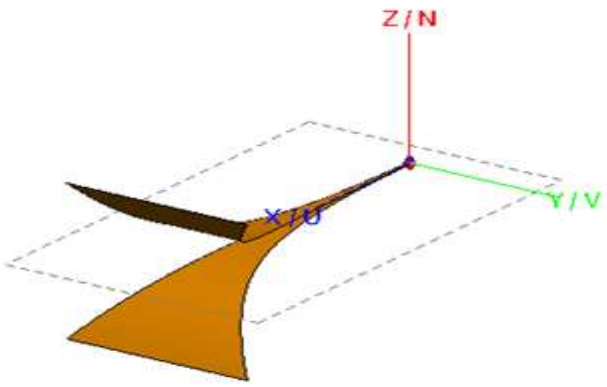

Figure 5. 1: TEM120cm with 200 Ohm aperture 3D view

5.3 TEM120cm with 250 Ohm aperture design

The designed new antenna should operate for at least a decade with lowest frequency at **250 MHz.**

- The TEM horn antenna length should be not less than 1 λ
- Therefore, $\lambda = 300/250 = 1.2$ m or 120 cm
- Substituting Z_0 as 50 Ω, Z_{ap} as 250 Ω and L as 120cm in equation (5.1) we get the characteristics impedance of the TEM horn is given as

$$Z(x) = 50\, e^{0.01341x} \quad \text{(cm)} \tag{5.7}$$

- Substituting d_0 as 0.2 cm, $d_L = \lambda/2 = 60$ cm and L as 120cm in equation (5.2) we get the separation between the upper and lower conductors of the TEM horn as a function of x as

$$d(x) = 0.2\, e^{0.04753x} \quad \text{(cm)} \tag{5.8}$$

- Substituting Z_{ap} as 250 Ω, $d(x) = 0.2\, e^{0.04753x}$ and $Z(x) = 50\, e^{0.01341x}$ in equation (5.3) we get the width of the TEM horn as a function of x as

$$w(x) = 1.0 * e^{0.03412x} \text{ (cm)} \tag{5.9}$$

The TEM horn is simulated in FEKO in a similar way as described in Appendix C and the 3D view of the simulated TEM horn is shown in Figure 5.2.

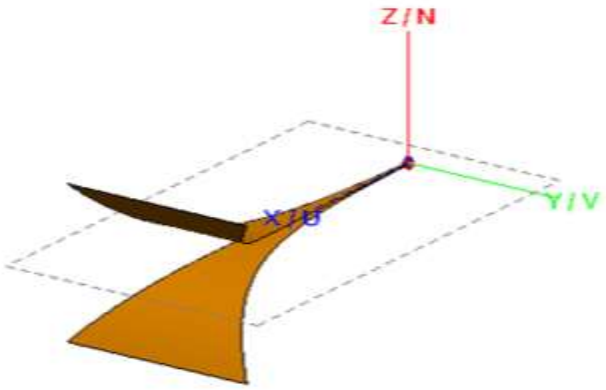

Figure 5. 2: TEM120cm with 250 Ohm aperture 3D view

5.4 TEM120cm with 377 Ohm aperture design

The designed new antenna should operate for at least a decade with lowest frequency at **250 MHz.**

- The TEM horn antenna length should be not less than 1 λ
- Therefore, $\lambda = 300/250 = 1.2$ m or 120 cm
- Substituting Z_0 as 50 Ω, Z_{ap} as 377 Ω and L as 120cm in equation (5.1) we get the characteristics impedance of the TEM horn is given as

$$Z(x) = 50\, e^{0.016835x} \quad (cm) \tag{5.10}$$

- Substituting d_0 as 0.2 cm, $d_L = \lambda/2 = 60$ cm and L as 120cm in equation (5.2) we get the separation between the upper and lower conductors of the TEM horn as a function of x as

$$d(x) = 0.2\, e^{0.04753x} \quad (cm) \tag{5.11}$$

- Substituting Z_{ap} as 377 Ω, $d(x) = 0.2\, e^{0.04753x}$ and $Z(x) = 50\, e^{0.016835x}$ in equation (5.3) we get the width of the TEM horn as a function of x as

$$w(x) = 1.508 * e^{0.030695x} \ (cm) \tag{5.12}$$

The TEM horn is simulated in FEKO in a similar way as described in Appendix C and the 3D view of the simulated TEM horn is shown in Figure 5.3.

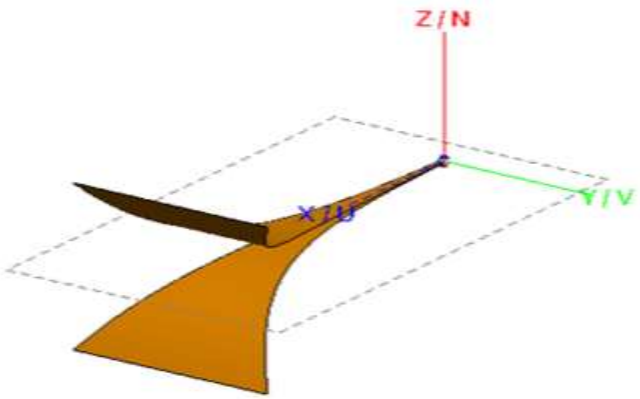

Figure 5. 3: TEM120cm with 377 Ohm aperture 3D view

5.5 TEM60cm with 200 Ohm aperture design

The designed new antenna should operate for at least a decade with lowest frequency at **500 MHz.**

- The TEM horn antenna length should be not less than 1 λ
- Therefore, $\lambda = 300/500 = 0.6$ m or 60 cm
- Substituting Z_0 as 50 Ω, Z_{ap} as 200 Ω and L as 60cm in equation (5.1) we get the characteristics impedance of the TEM horn is given as

$$Z(x) = 50\, e^{0.0231x} \quad (cm) \tag{5.13}$$

- Substituting d_0 as 0.2 cm, $d_L = \lambda/2 = 30$ cm and L as 60cm in equation (5.2) we get the separation between the upper and lower conductors of the TEM horn as a function of x as

$$d(x) = 0.2\, e^{0.0835x} \quad (cm) \tag{5.14}$$

- Substituting Z_{ap} as 200 Ω, $d(x) = 0.2\, e^{0.0835x}$ and $Z(x) = 50\, e^{0.0231x}$ in equation (5.3) we get the width of the TEM horn as a function of x as

$$w(x) = 0.8 * e^{0.0604\,x} \ (cm) \tag{5.15}$$

The TEM horn is simulated in FEKO in a similar way as described in Appendix C and the 3D view of the simulated TEM horn is shown in Figure 5.4.

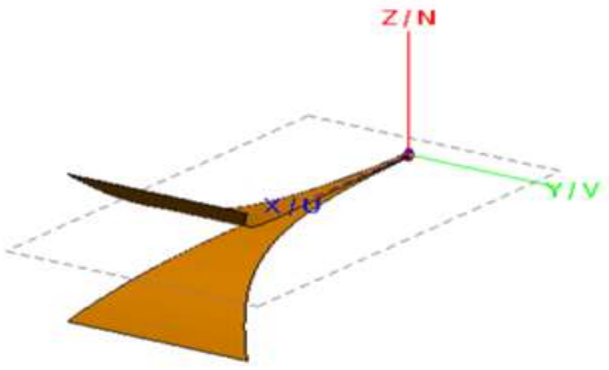

Figure 5. 4: TEM60cm with 200 Ohm aperture 3D view

5.6 TEM60cm with 250 Ohm aperture design

The designed new antenna should operate for at least a decade with lowest frequency at **500 MHz.**

- The TEM horn antenna length should be not less than 1 λ
- Therefore, $\lambda = 300/500 = 0.6$ m or 60 cm
- Substituting Z_0 as 50 Ω, Z_{ap} as 250 Ω and L as 60cm in equation (5.1) we get the characteristics impedance of the TEM horn is given as

$$Z(x) = 50\, e^{0.0268x} \quad (cm) \tag{5.16}$$

- Substituting d_0 as 0.2 cm, $d_L = \lambda/2 = 30$ cm and L as 60cm in equation (5.2) we get the separation between the upper and lower conductors of the TEM horn as a function of x as

$$d(x) = 0.2\, e^{0.0835x} \quad (cm) \tag{5.17}$$

- Substituting Z_{ap} as 250 Ω, $d(x) = 0.2\, e^{0.0835x}$ and $Z(x) = 50\, e^{0.0268x}$ in equation (5.3) we get the width of the TEM horn as a function of x as

$$w(x) = 1.0 * e^{0.0567x} \ (cm) \tag{5.18}$$

The TEM horn is simulated in FEKO in a similar way as described in Appendix C and the 3D view of the simulated TEM horn is shown in Figure 5.5.

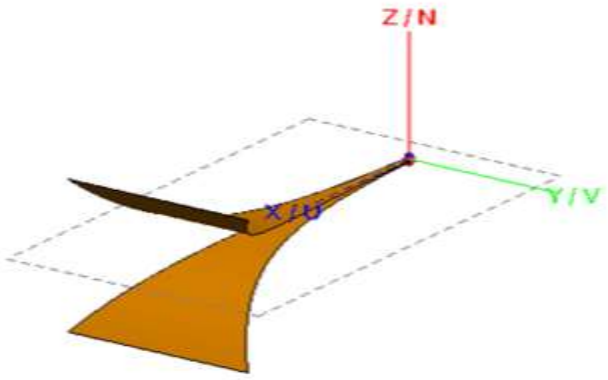

Figure 5. 5: TEM60cm with 250 Ohm aperture 3D view

5.7 TEM60cm with 377 Ohm aperture design

The designed new antenna should operate for at least a decade with lowest frequency at **500 MHz.**

- The TEM horn antenna length should be not less than 1 λ
- Therefore, $\lambda = 300/500 = 0.6$ m or 60 cm
- Substituting Z_0 as 50 Ω, Z_{ap} as 377 Ω and L as 60cm in equation (5.1) we get the characteristics impedance of the TEM horn is given as

$$Z(x) = 50\, e^{0.03367x} \quad (cm) \tag{5.19}$$

- Substituting d_0 as 0.2 cm, $d_L = \lambda/2 = 30$ cm and L as 60cm in equation (5.2) we get the separation between the upper and lower conductors of the TEM horn as a function of x as

$$d(x) = 0.2\, e^{0.0835x} \quad (cm) \tag{5.20}$$

- Substituting Z_{ap} as 377 Ω, $d(x) = 0.2\, e^{0.0835x}$ and $Z(x) = 50\, e^{0.0268x}$ in equation (5.3) we get the width of the TEM horn as a function of x as

$$w(x) = 1.508 * e^{0.04983x} \ (cm) \tag{5.21}$$

The TEM horn is simulated in FEKO in a similar way as described in Appendix C and the 3D view of the simulated TEM horn is shown in Figure 5.6.

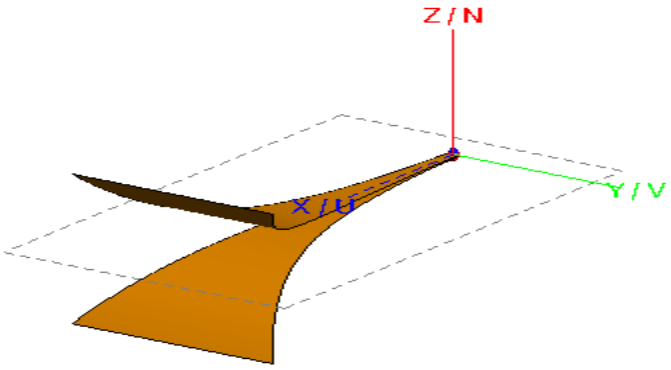

Figure 5. 6: TEM60cm with 377 Ohm aperture 3D view

CHAPTER VI

Voltage Standing Wave Ratio Simulation Results

6.1 Voltage Standing Wave Ratio(VSWR)

VSWR is defined by equation 6.1.

$$\text{VSWR} = \frac{1+|\Gamma|}{1-|\Gamma|} \tag{6.1}$$

Where Γ is reflection coefficient and is given by equation (6.2),

$$\Gamma = \frac{V_{rev}}{V_{fwd}} = \sqrt{\frac{P_{rev}}{P_{fwd}}} = \frac{Z_L - Z_0}{Z_L + Z_0} \tag{6.2}$$

Where,

- V_{rev} is the reflected voltage wave and V_{fwd} is the forward voltage wave.
- P_{rev} is the reflected power and P_{fwd} is the forward power.
- Z_L is the load impedance and Z_0 is the reference characteristics impedance

An excitation voltage of amplitude = 1 V,phase = 0^0 and reference impedance = 50 Ω is applied to the "feed" of TEM horn antennas via a wire port and the VSWR of the designed TEM horn antennas is simulated and it is found that the VSWR is less than 2 over an ultra-wide frequency range within the frequency range of interest.

By frequency range of interest we mean, TEM120cm with 200,250 and 377 Ohm aperture impedance is designed to operate at least within a decade frequency range with the lowest frequency at 250 MHz and the highest frequency at 2500 MHz and TEM60cm with 200,250 and 377 Ohm aperture impedance is designed to operate within a decade frequency range with the lowest frequency at 500 MHz and the highest frequency at 5000 MHz.

VSWR less than 2 is mathematically expressed by equation 6.3.

$$\text{VSWR} = \frac{1+|\Gamma|}{1-|\Gamma|} < 2 \tag{6.3}$$

After a little algebraic manipulation and solving for Γ we get,

$$|\Gamma| < 1/3 \tag{6.4}$$

Further simplification results in,

$$-\frac{1}{3} < \Gamma < \frac{1}{3} \tag{6.5}$$

The above analysis is interpreted to mean less than 11.1% of the transmitted power is reflected back to the "feed", which means that the designed TEM horn antennas can effectively transmit over the frequency range of interest.

See Table 6.1 for the summary of VSWR simulation results.

Table 6. 1: Summary of VSWR simulation results

Item #	Antenna length (cm)	Aperture impedance (Ohm)	f_L , Lower-cutoff frequency (MHz)	f_H ,Higher Frequency (MHz)	b_w , Fractional bandwidth	VSWR result	Frequency range (MHz)
1	120	200	250	2500	1.63	~2	250-500
						< 2	500-2500
						< 1.66	2500-3000
2	120	250	250	2500	1.63	~2	250-500
						< 2	500-2500
						< 1.53	2500-3000
3	120	377	250	2500	1.63	~2	250-500
						< 2	500-2500
						< 1.91	2500-3000
4	60	200	500	5000	1.63	< 2	500-2000
						< 2	2000-5000
						< 2.24	5000-6000
5	60	250	500	5000	1.63	< 2	500-2000
						< 2	2000-5000
						< 2.38	5000-6000
6	60	377	500	5000	1.63	< 2	500-2000
						< 2.86	2000-5000
						< 3.52	5000-6000

Due to limitation of student version of FEKO, it is not possible to simulate the VSWR in a single plot over the entire frequency range so the VSWR is simulated with the possible frequency range as depicted in Figure 6.1 to 6.6.

Due to the fact that GPR antennas are usually situated in the vicinity of the ground, their requirements are different from those of antennas operating in free space. Their design criteria can also vary depending on the application.

The TEM horn antenna is required to couple the electromagnetic signal into the ground so the most important antenna parameter that should be simulated is VSWR.

6.2 VSWR of TEM120cm with 200,250 and 377 Ohm aperture impedance

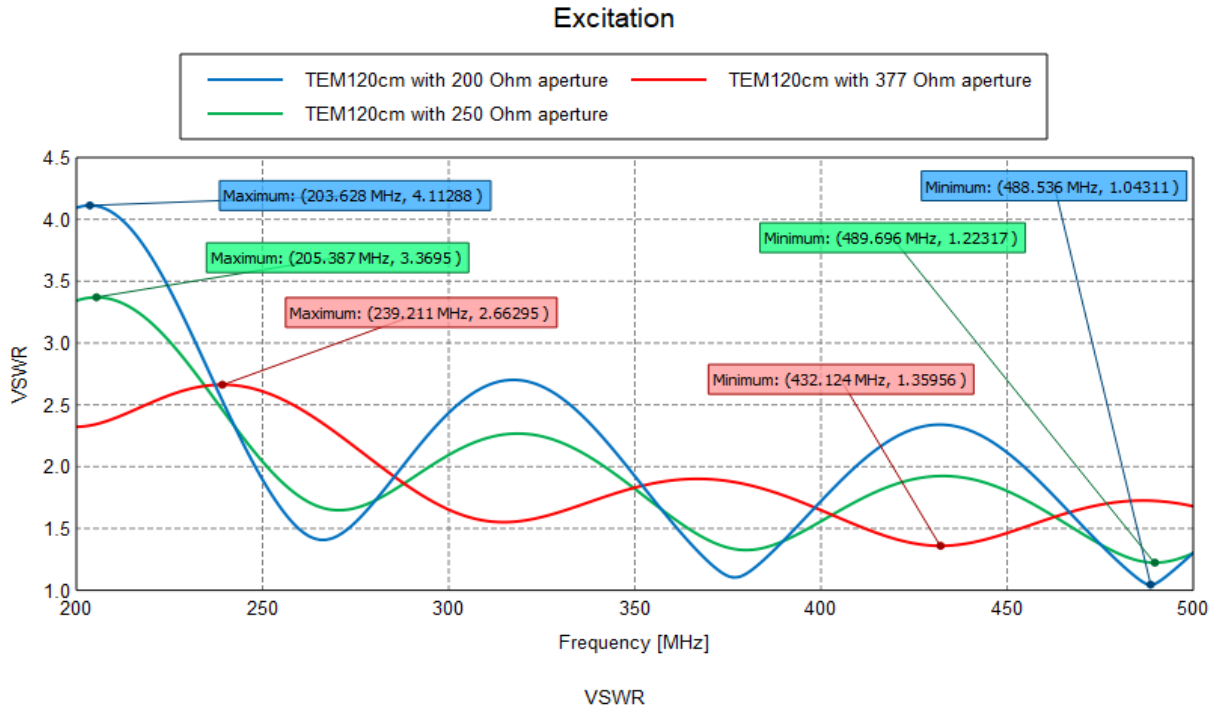

Figure 6. 1: VSWR of TEM120cm with 200,250 and 377 Ohm aperture impedance from 200 MHz to 500 MHz

From Figure 6.1, it can be seen that TEM120cm with 200,250 and 377 Ohm aperture impedance have comparable VSWR oscillating on VSWR ~2 from 250 MHz to 500 MHz.

From Figure 6.2 to Figure 6.3 in the following pages we can see that TEM120cm each with aperture impedance of 200 and 250 Ohm designed in double exponential approach have less VSWR than TEM horn antenna with 377 Ohm aperture impedance of similar size as the frequency of operation increase which confirms that setting aperture impedance of TEM horn antenna to 377 Ohm does not assure the best matching performance.

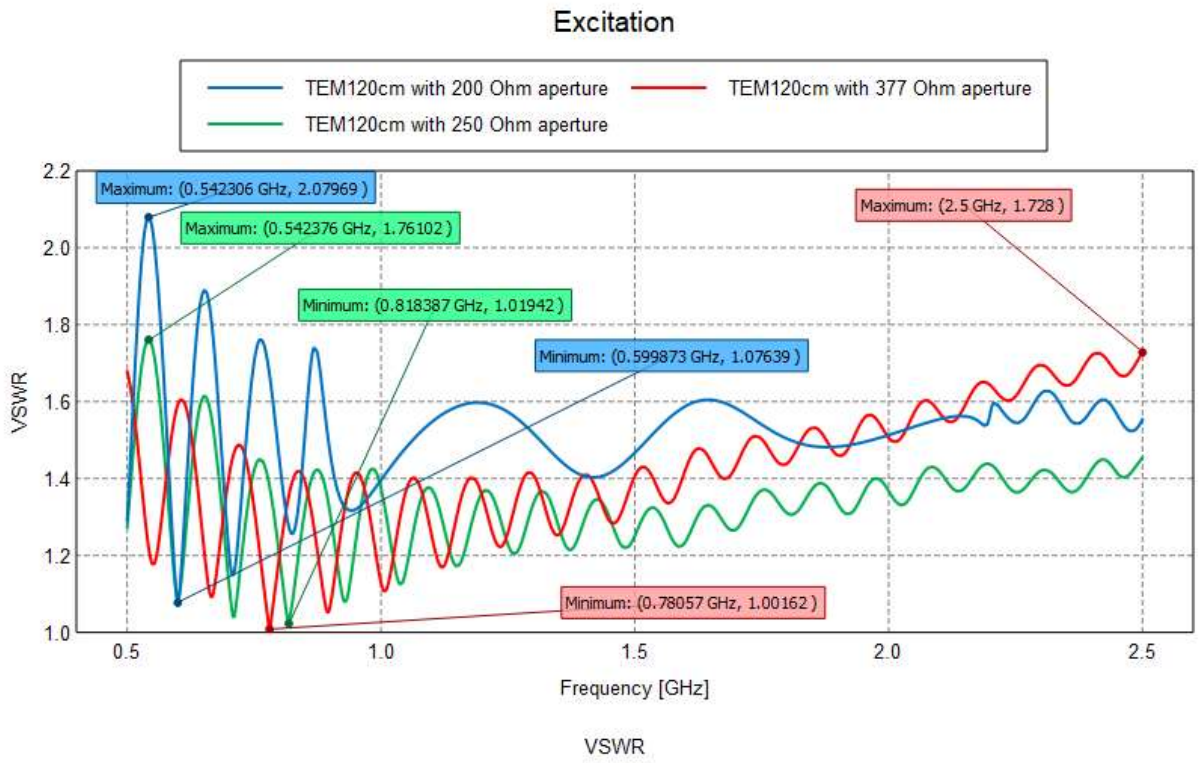

Figure 6. 2: VSWR of TEM120cm with 200,250 and 377 Ohm aperture impedance from 500 MHz to 2500 MHz

377 Ohm is not the best aperture impedance for TEM horn antenna matching to free space.

From Figure 6.2,it can be seen that TEM120cm with 250 Ohm aperture impedance has less VSWR than TEM120cm with 200 Ohm and TEM120cm with 377 Ohm aperture impedance from 1500 MHz to 2500 MHz. This is due to the feedline width i.e. 1 cm of TEM120cm with 250 Ohm which makes better matching in the frequency range 1500 MHz to 2500 MHz.

TEM120cm with 200 Ohm aperture has less VSWR than TEM120cm with 377 Ohm from 2000 MHz to 2500 MHz.

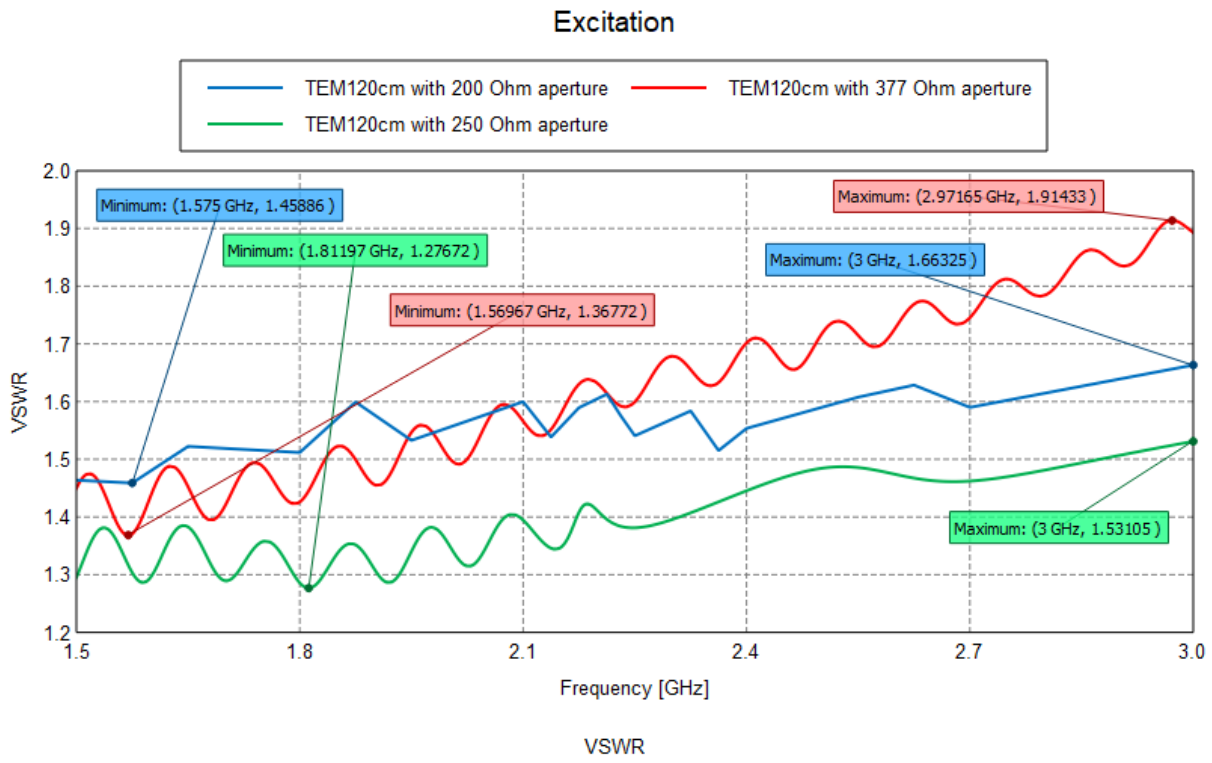

Figure 6. 3: VSWR of TEM120cm with 200,250 and 377 Ohm aperture impedance from 1500 MHz to 3000 MHz

From Figure 6.3,it can be seen that TEM120cm with 250 Ohm aperture impedance have less VSWR than TEM120cm with 200 Ohm and TEM120cm with 377 Ohm aperture impedance from 1500 MHz to 3000 MHz.

Also from 2000 MHz to 3000 MHz TEM120cm with 200 Ohm aperture have less VSWR than TEM120cm with 377 Ohm.

From 6.3, we can see that as the frequency of operation increases the VSWR difference between TEM120cm horn antennas with aperture impedance of 200 and 250 on one hand and 377 Ohm on the other hand increases and the VSWR of TEM120cm with 377 Ohm is increasing significantly as the frequency of operation increases which confirms that setting aperture impedance of TEM horn antenna to 377 Ohm does not assure the best matching performance.

6.3 VSWR of TEM60cm with 200,250 and 377 Ohm aperture impedance

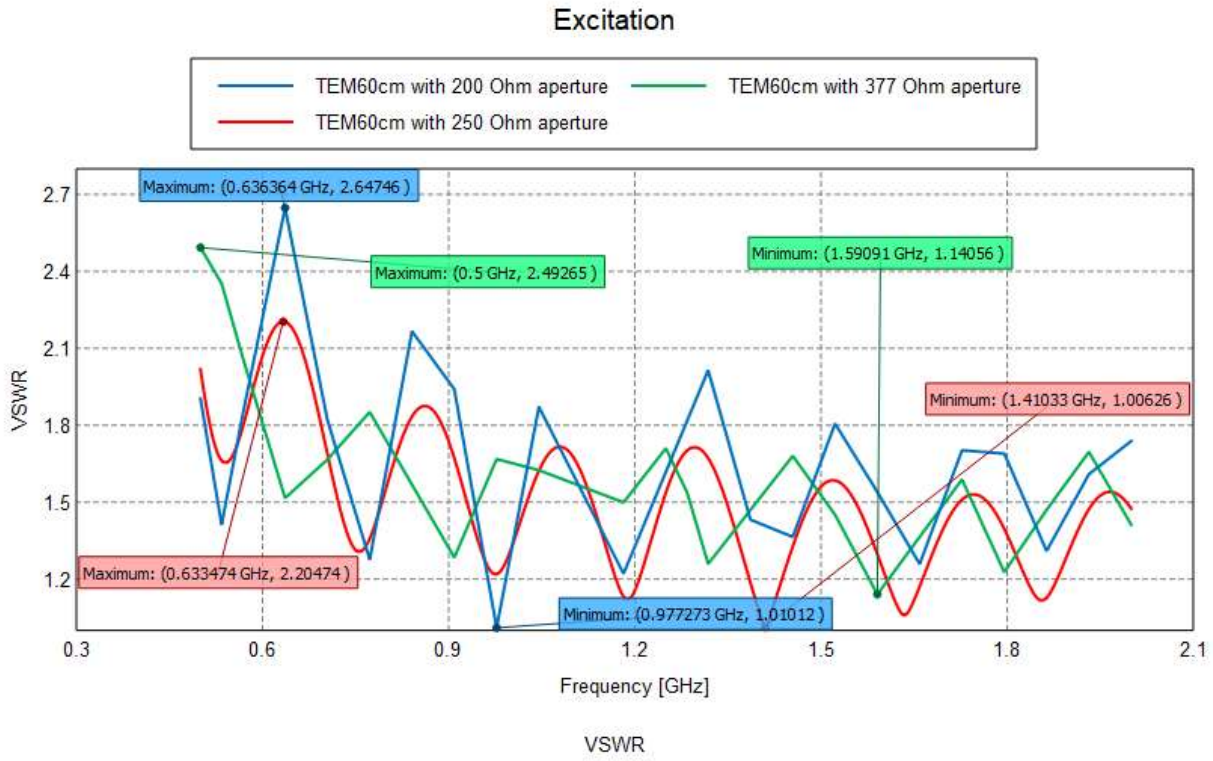

Figure 6. 4: VSWR of TEM60cm with 200,250 and 377 Ohm aperture impedance from 500 MHz to 2000 MHz

From Figure 6.4, it can be seen that TEM60cm with 200,250 and 377 Ohm aperture impedance have comparable VSWR oscillating on VSWR ~2 from 500 MHz to 2000 MHz.

From Figure 6.5 to Figure 6.6 in the following pages we can see that TEM60cm with aperture impedance of 200 and 250 Ohm designed in double exponential approach have less VSWR than TEM horn antenna with 377 Ohm aperture impedance of similar size as the frequency of operation increase which confirms that setting aperture impedance of TEM horn antenna to 377 Ohm does not assure the best matching performance.

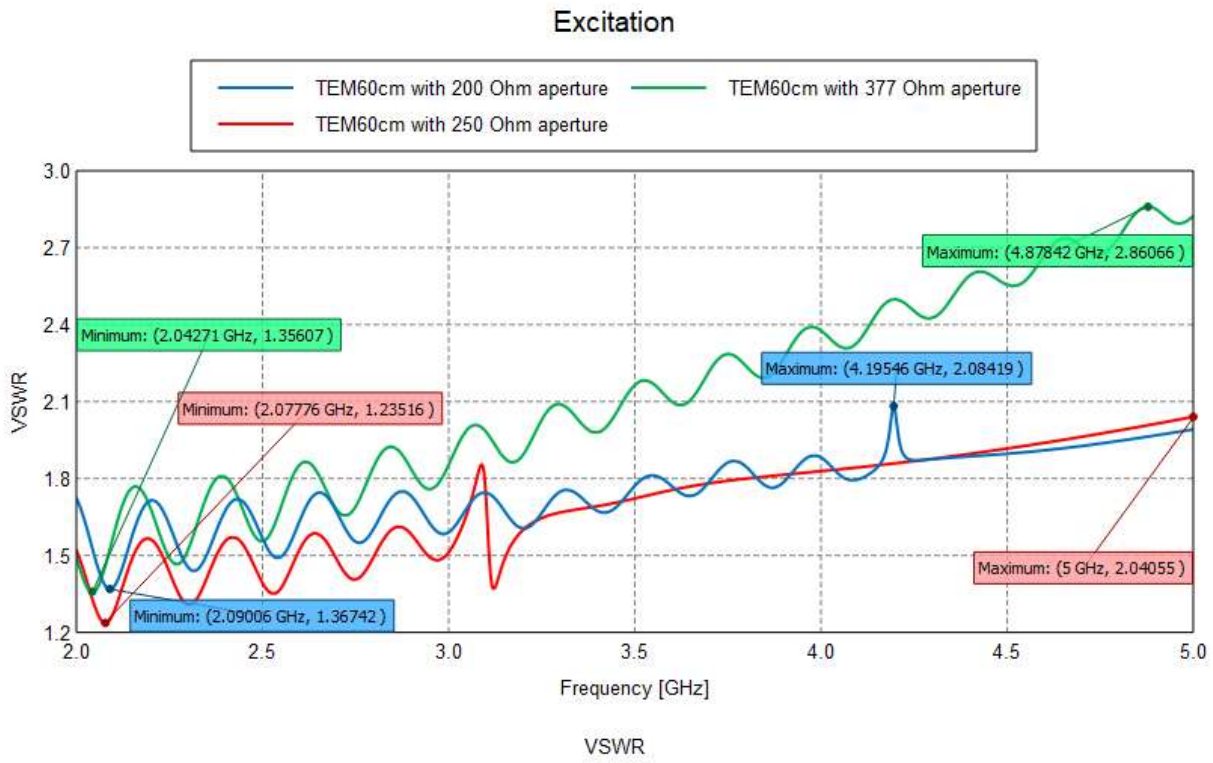

Figure 6. 5: VSWR of TEM60cm with 200,250 and 377 Ohm aperture impedance from 2000 MHz to 5000 MHz

377 Ohm is not the best aperture impedance for TEM horn antenna matching to free space.

From Figure 6.5,it can be seen that TEM60cm with 200 and 250 Ohm aperture impedance have comparable VWSR with each other and thay have less VSWR than TEM60cm with 377 Ohm aperture impedance from 2500 MHz to 5000 MHz which confirms that setting aperture impedance of TEM horn antenna to 377 Ohm does not assure the best matching performance.

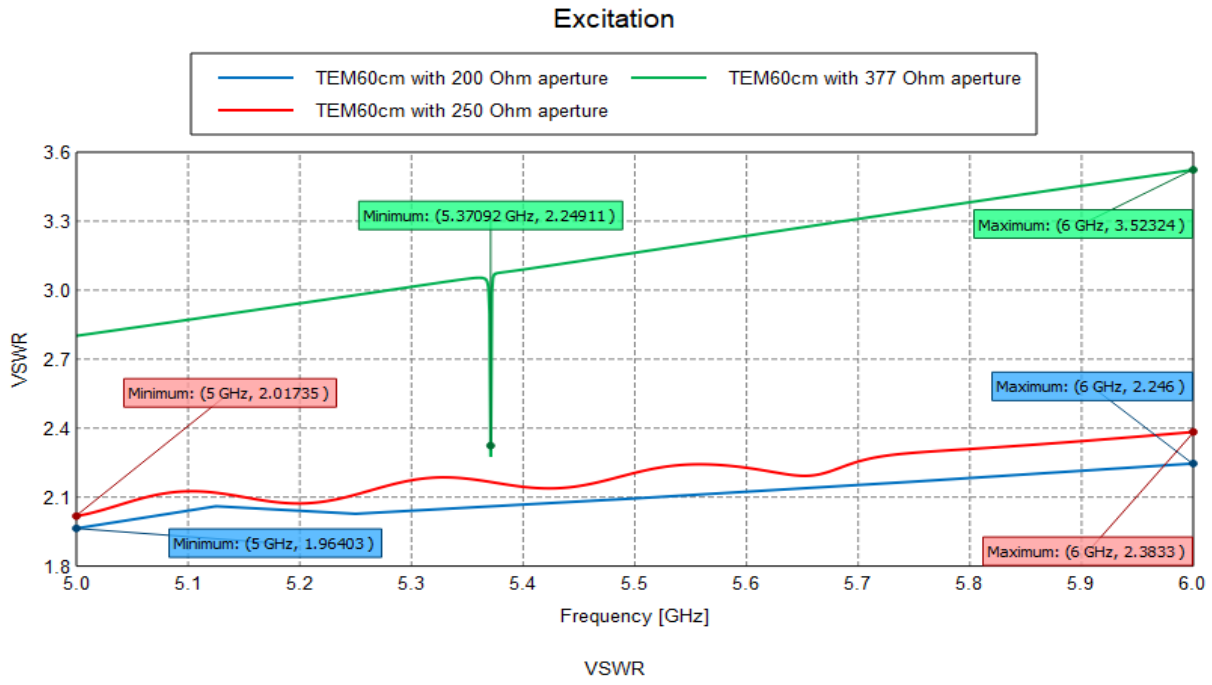

Figure 6. 6: VSWR of TEM60cm with 200,250 and 377 Ohm aperture impedance from 5000 MHz to 6000 MHz

From Figure 6.6,it can be seen that TEM60cm with 200 and 250 Ohm aperture impedance have comparable VSWR with each other and thay have less VSWR than TEM60cm with 377 Ohm aperture impedance from 5000 MHz to 6000 MHz.

From 6.6, we can see that as the frequency of operation increases the VSWR difference between TEM120cm horn antennas with aperture impedance of 200 and 250 Ohm on one hand and 377 Ohm on the other hand increases and the VSWR of TEM120cm with 377 Ohm is increasing significantly as the frequency of operation increases which confirms that setting aperture impedance of TEM horn antenna to 377 Ohm does not assure the best matching performance.

In Figure 6.6,the irregularity at 5.37092 GHz is a result of the simulation software meshing.

CHAPTER VII

Conclusions and Recommendations for Future works

7.1 Conclusions

The state of the art approach of setting the aperture impedance of TEM horn antenna to 377 Ohm does not assure the best matching performance.

TEM60cm and TEM120cm with aperture impedance of 200 and 250 Ohm which are designed via double exponential approach have less VSWR than 377 Ohm aperture TEM horn antenna of the same size over an ultra-wide frequency range.

All of the designed TEM horn antennas fulfill the criterion of being UWB antenna described in chapter 3 by equation 3.2.

As the length of TEM horn antenna increases its lower cut-off frequency decreases and can be used for low frequency applications which can penetrate deeply in to the ground. As the length of the TEM horn decreases its lower cut-off frequency increases and can be used for high frequency applications with limited penetration depth. This indicates that the lower cut-off frequency is mainly governed by the dimension of the antenna and is inversely proportional to the dimension of the TEM horn antenna.

TEM120cm horn antenna with aperture impedance of 250 Ohm has lower VSWR than TEM120cm horn antenna with aperture impedance of 200 Ohm as the frequency increase.

TEM60cm horn antenna with aperture impedance of 200 Ohm has lower VSWR than TEM60cm horn antenna with aperture impedance of 250 Ohm as frequency increase.

As we can see from Appendix C,FEKO simulation software is found to be a suitable and user friendly software for this thesis.

7.2 Recommendations for Future works

A study can be conducted to find the exact relationship between aperture impedance and VSWR of TEM horn antenna.

In the future, cross coupling between the transmitter and receiver of TEM horn antennas of GPR system can be simulated by filling different dielectric materials between the upper and lower conductors of the TEM horn antennas and find the best dielectric material which reduces cross coupling.

It is anticipated that the designed TEM horn antennas can be used for impulse GPR applications.

REFERENCES

[1] A. A. Lestari, A.G. Yarovoy, and L.P. Ligthart, "Analysis and Design of Improved Antennas for GPR," *Subsurface Sensing Technologies and Applications* vol. 3, no. 4,pp. 295-326, Oct 2002

[2] R. V. de Jongh,A. G. Yarovoy,L. P. Ligthart,I. V. Kaploun, and A. D. Schukin, "Design and analysis of new GPR antenna concepts," *Tijdschrift-Nederlands Elektronica En Radiogenootschap*,pp. 26-32, 1999

[3] H. Y. Pao, and A.J. Poggio, "Design of a TEM Waveguide for Ultra-wideband Applications," *IEEE Antennas and Propagation Society International Symposium*, vol. 3, pp. 1574-1577,1999

[4] C. A. Grosvenor, R. T. Johnk, D. R. Novotny,N. Canales,B. Davis, and J. Veneman," TEM Horn Antenna Design Principles," *Technical Note(NIST TN)* 1544,Jan 2007

[5] A. A. Lestari, A. G. Yarovoy, and L. P. Ligthart, "Adaptive Wire Bow-Tie Antenna for GPR Applications," *IEEE transactions on antennas and propagation*, vol. 53, no. 5,pp. 1745-1754,May,2005

[6] M. Kanda, "The Effects of Resistive Loading of TEM Horns," *IEEE transactions on electromagnetic compatibility*, vol. EMC-24, no. 2, pp. 245-255,May 1982

[7] A. Yarovoy, and J. Zijderveld, "Analysis of Radiation from a Dielectric Wedge Antenna," *In Ultra-wideband, short-pulse electromagnetics 7*,New York: Springer,2007,pp. 325-333

[8] A. G. Yarovoy, A.D. Schukin and L. P. Ligthart, "Development of dielectric filled TEM-horn,"2000

[9] D. A. Kolokotronis, Y. Huang and J. T. Bang, Liverpool,"Design of TEM Horn Antennas for Impulse Radar," *IEEE High Frequency Postgraduate Student Colloquium*, pp. 120-126, September 17, 1999

[10] K. H. Chung,S. H. Pyun,S. Y. Chung and J. H. Choi, "Design of a Wideband TEM Horn Antenna," *In IEEE Antennas and Propagation Society International Symposium. Digest. Held in conjunction with: USNC/CNC/URSI North American Radio Sci. Meeting* ,2003,vol. 1,pp. 229-232

[11] K. H. Chung, S. H. Pyun, and J. H. Choi, "Design of an Ultra-wideband TEM Horn Antenna With a Microstrip-Type Balun," *IEEE Transactions on Antennas and Propagation*, vol. 53, no. 10, pp. 3410-3413,October 2005

[12] S. Bassam and J. Rashed-Mohassel, "A Chebyshev Tapered TEM Horn Antenna," *PIERS online*, vol. 2, no. 6, pp. 706-709,2006

[13] Y. Huang, M. Nakhkashl and J. T. Zhang, "A Dielectric Material Loaded TEM Horn Antenna,"pp. 489-492,2003

[14] C.P. Kao,J. Li, R. Liu and Y. Cai,"Design and analysis of UWB TEM horn antenna for ground penetrating radar applications," *In IGARSS IEEE*, 2008,vol. 4, pp. IV-569

[15] A. P. Annan, "Electromagnetic principles of ground penetrating radar,"2009

[16] D. J. Daniels, "Surface-penetrating radar," *Electronics & Communication Engineering Journal 8*,no. 4,pp. 165-182,Aug 1996

[17] E. C. Utsi, *Ground Penetrating Radar, Theory and Practice*, Butterworth-Heinemann,2017

[18] D. Goodman and S. Piro, *GPR Remote Sensing in Archaeology*, New York: Springer,2013

[19] A. A. Lestari,"Antennas for Improved Ground Penetrating Radar: Modeling Tools, Analysis and Design," Ph.D. dissertation,2003

[20] J. H. Bungey, "Sub-surface radar testing of concrete: a review," *Construction and Building materials 18*, no. 1,pp. 1-8,2004

[21] H. M. Jol, *Ground Penetrating Radar: Theory and Applications*, Elsevier,2009

[22] B. Scheers, "Ultra-wideband ground penetrating radar with Application to the detection of anti-personnel," Royal Military Academy, Brussels, Mar 2001

[23] A. G. Yarovoy, P. van Genderen and L.P. Ligthart, "Ultra-wideband ground penetrating impulse radar," *In Ultra-wideband, Short-Pulse Electromagnetics 5*, 2002,pp. 183-189

[24] M. Robinson, C. Bristow, J. McKinley and A. Ruffell, "Ground Penetrating Radar," *Geomorphological Techniques*, Part 1, Sec. 5.5 ,2013

[25] D. J. Daniels, "A review of GPR for landmine detection," *Sensing and Imaging* , vol. 7,no. 3,pp. 90-123,Sep, 2006

[26] C. A. Balanis, *Antenna Theory, Analysis and Design*,3rd ed., John Wiley & Sons,2005

[27] J. D. Kraus and D. A. Fleisch, Electromagnetics with Applications, 5th ed.,WCB/McGraw-Hill,1999

[28] F. B. Gross, *Frontiers in antennas: Next generation design & engineering*, New York: McGraw-Hill Professional, 2011

[29] J. Ali,N. Abdullah,M. Y. Ismail, E. Mohd, and S. M. Shah, "Ultra-Wideband Antenna Design for GPR Applications: A Review," *IJACSA*,vol. 8, no.7, 2017

[30] H. G. Schantz, *The Art and Science of Ultra-wideband Antennas*,2nd ed.,Artech House,2015

[31] H. G. Schantz, "Introduction to Ultra-Wideband Antennas," *In IEEE Conference on Ultra-Wideband Systems and Technologies*, 2003,pp. 1-9

[32] H. G. Schantz, "Dispersion and UWB Antennas," *IEEE International Workshop on Ultra-Wideband Systems Joint with Conference on Ultra Wideband Systems and Technologies. Joint UWBST & IWUWBS*,2004,pp. 161-165

[33] R. T. Lee and G. S. Smith, "On the Characteristic Impedance of the TEM Horn Antenna," *IEEE transactions on antennas and propagation*, vol. 52, no. 1,pp. 315-318,January,2004

[34] R. T. Lee and G. S. Smith, "A design study for the basic TEM horn antenna," *IEEE Antennas and Propagation Magazine*, vol. 46, no. 1, pp. 86-92,February 2004

[35] C. Yeh and F. I. Shimabukuro, *The Essence of Dielectric Waveguides*,New York: Springer, 2008

[36] Altair HyperWorks, "Characteristic Mode Analysis for Ultra-Wideband Antenna Design," *Application Sheet*,2019

[37] B. Scheers, M. Piette and A. Vander Vorst, "Development of dielectric-filled TEM horn antennas for UWB GPR," *In Millennium Conference on Antennas & Propagation*, 2000,pp. 187

[38] E. K. Miller, "Time-Domain Measurements in Electromagnetics," *Springer Science & Business Media*, 1986

[39] I. L. Gallon and D. V. Giri, "Design of a Certain Class of Broad Band Dipole Antennas," *Sensor and Simulation Notes*, Note 570, Mar 2015

[40] M. Nakhkash and Y. Huang, "Directive Wideband TEM Horn Antenna for Precise Free-Space Measurements," *In IEEE Conference Digest Conference on Precision Electromagnetic Measurements*,2002,pp. 140-141

[41] M. Khorshidi and M. Kamyab,"New exponential TEM horn antenna with binomial impedance taper," *AEU-International Journal of Electronics and Communications 64*,no. 11,pp. 1073-1077, 2010

[42] A. R. Mallahzadeh and F. Karshenas,"Modified TEM Horn Antenna for Broadband Applications," *Progress In Electromagnetics Research, PIER 90*, pp. 105-119, 2009

[43] K. Harima,"Numerical estimation for TEM horn antennas with transmission line taper shapes,"*IEICE Communications Express,* vol.6, no.9, pp. 560–565,2017

[44] J. Stile. "Tapered Lines," The University of Kansa, Dep't of EEC, Apr,2010. Available: http://www.ittc.ku.edu/~jstiles/723/handouts/Tapered%20Lines.pdf

[45] C. A. Grosvenor, R. Johnk, D. Novotny, N. Canales, "TEM-horn antennas: A promising new technology for compliance testing," *IEEE International Symposium on Electromagnetic Compatibility*,2004, vol. 3, pp. 913-918

[46] S. Yin, Y. Sun, and P. Li, "A New Design of TEM Horn Antenna Based on Ultra-Wideband Broken Line," *IEEE Progress in Electromagnetic Research Symposium (PIERS)*,2001, pp. 4375-4378

[47] D. Fleisch, *A student's guide to Maxwell's equations*, Cambridge University Press; Jan 2008

[48] Altair HyperWorks, User Guide: Altair FEKO 2019.3,2019

Appendix A

The wave equation

Like all good mathematical operators, $\vec{\nabla}$(del) is an action waiting to happen. Just as $\surd$ tells you to take the square root of anything that appears under its roof, $\vec{\nabla}$ is an instruction to take derivatives in three directions. Specifically [47],

$$\vec{\nabla} = \hat{\imath}\,\frac{\partial}{\partial x} + \hat{\jmath}\,\frac{\partial}{\partial y} + \hat{k}\,\frac{\partial}{\partial z} \tag{A.1}$$

Where $\hat{\imath}$, $\hat{\jmath}$ and $\hat{k}$ are the unit vectors in the direction of the Cartesian coordinates x, y, and z.

With the differential form of Maxwell's Equations and several vector operator identities in hand, the trip to the wave equation is a short one. Begin by taking the curl of both sides of the differential form of Faraday's law [47],

$$\vec{\nabla} \times \left(\vec{\nabla} \times \vec{E}\right) = \vec{\nabla} \times \left(-\frac{\partial \vec{B}}{\partial t}\right) = -\frac{\partial\left(\vec{\nabla} \times \vec{B}\right)}{\partial t} \tag{A.2}$$

Notice that the curl and time derivatives have been interchanged in the final term; as in previous sections, the fields are assumed to be sufficiently smooth to permit this [47].

Another useful vector operator identity says that the curl of the curl of any vector field equals the gradient of the divergence of the field minus the Laplacian of the field [47]:

$$\vec{\nabla} \times \left(\vec{\nabla} \times \vec{A}\right) = \vec{\nabla} \times \left(\vec{\nabla} \circ \vec{A}\right) - \nabla^2 \vec{A} \tag{A.3}$$

This relation uses a vector version of the Laplacian operator that is constructed by applying the Laplacian to the components of a vector field [47]:

$$\nabla^2 \vec{A} = \frac{\partial^2 A_x}{\partial x^2} + \frac{\partial^2 A_y}{\partial y^2} + \frac{\partial^2 A_z}{\partial z^2} \quad \text{(Cartesian)} \tag{A.4}$$

Thus,

$$\vec{\nabla} \times \left(\vec{\nabla} \times \vec{E}\right) = \vec{\nabla} \times \left(\vec{\nabla} \circ \vec{E}\right) - \nabla^2 \vec{E} = -\frac{\partial\left(\vec{\nabla} \times \vec{B}\right)}{\partial t} \tag{A.5}$$

However, you know the curl of the magnetic field from the differential form of the Ampere–Maxwell law [47]:

$$\vec{\nabla} \times \vec{B} = \mu_0 \left(\vec{J} + \varepsilon_0 \frac{\partial \vec{E}}{\partial t} \right) \tag{A.6}$$

So,

$$\vec{\nabla} \times \left(\vec{\nabla} \times \vec{E} \right) = \vec{\nabla} \times \left(\vec{\nabla} \circ \vec{E} \right) - \nabla^2 \vec{E} = - \frac{\partial \left(\mu_0 \left(\vec{J} + \varepsilon_0 \left(\partial \vec{E} / \partial t \right) \right) \right)}{\partial t} \tag{A.7}$$

This looks difficult, but one simplification can be achieved using Gauss's law for electric fields [47]:

$$\vec{\nabla} \circ \vec{E} = \frac{\rho}{\varepsilon_0} \tag{A.8}$$

which means,

$$\begin{aligned} \vec{\nabla} \times \left(\vec{\nabla} \times \vec{E} \right) = \vec{\nabla} \left(\frac{\rho}{\varepsilon_0} \right) - \nabla^2 \vec{E} &= - \frac{\partial \left(\mu_0 \left(\vec{J} + \varepsilon_0 \left(\partial \vec{E} / \partial t \right) \right) \right)}{\partial t} \\ &= -\mu_0 \frac{\partial \vec{J}}{\partial t} - \mu_0 \varepsilon_0 \frac{\partial^2 \vec{E}}{\partial t^2} \end{aligned} \tag{A.9}$$

Gathering terms containing the electric field on the left side of this equation gives

$$\nabla^2 \vec{E} - \mu_0 \varepsilon_0 \frac{\partial^2 \vec{E}}{\partial t^2} = \vec{\nabla} \left(\frac{\rho}{\varepsilon_0} \right) + \mu_0 \frac{\partial \vec{J}}{\partial t} \tag{A.10}$$

In a charge- and current-free region, $\rho = 0$ and $\vec{J} = 0$

$$\nabla^2 \vec{E} = \mu_0 \varepsilon_0 \frac{\partial^2 \vec{E}}{\partial t^2} \tag{A.11}$$

This is a linear, second-order, homogeneous partial differential equation that describes an electric field that travels from one location to another – in short, a propagating wave. Here is a quick reminder of the meaning of each of the characteristics of the wave equation [47]:

Linear: The time and space derivatives of the wave function ($\vec{E}$ in this case) appear to the first power and without cross terms.

Second-order: The highest derivative present is the second derivative.

Homogeneous: All terms involve the wave function or its derivatives, so no forcing or source terms are present.

Partial: The wave function is a function of multiple variables (space and time in this case). A similar analysis beginning with the curl of both sides of the Ampere–Maxwell law leads to [47].

$$\nabla^2\vec{B} = \mu_0\varepsilon_0 \frac{\partial^2\vec{B}}{\partial t^2} \tag{A.12}$$

which is identical in form to the wave equation for the electric field.

This form of the wave equation doesn't just tell you that you have a wave – it provides the velocity of propagation as well. It is right there in the constants multiplying the time derivative, because the general form of the wave equation is this [47].

$$\nabla^2\vec{A} = \frac{1}{v^2}\frac{\partial^2\vec{A}}{\partial t^2} \tag{A.13}$$

where v is the speed of propagation of the wave. Thus, for the electric and magnetic fields

$$\frac{1}{v^2} = \mu_0\varepsilon_0 \tag{A.14}$$

or

$$v = \sqrt{\frac{1}{\mu_0\varepsilon_0}} \tag{A.15}$$

Inserting values for the magnetic permeability and electric permittivity of free space,

$$v = \sqrt{\frac{1}{[4\pi \times 10^{-7}\ \mathrm{m\ Kg/C^2}][8.8541878 \times 10^{-12}\ \mathrm{C^2 s^2/Kg\ m^3}]}} \tag{A.16}$$

or

$$v = \sqrt{8.987552\ \times 10^{16}\ \mathrm{m^2/s^2}} = 2.9979 \times\ 10^8\ \mathrm{m/s} \tag{A.17}$$

It was the agreement of the calculated velocity of propagation with the measured speed of light that caused Maxwell to write, ''light is an electromagnetic disturbance propagated through the field according to electromagnetic laws" [47].

Appendix B

FEKO Overview

FEKO is a comprehensive computational electromagnetics (CEM) software product used widely in the telecommunications, automotive, aerospace and defense industries [48].

The name FEKO is an abbreviation derived from the German phrase "**FE**ldberechnung bei **K**örpern mit beliebiger **O**berfläche" (field computations involving bodies of arbitrary shape). As the name suggests, FEKO can be used for various types of electromagnetic field analyses involving objects of arbitrary shapes. FEKO offers several frequency domain electromagnetic (EM) solution methods as well as a time domain method under a single license. Hybridisation of these methods enables efficient analysis of a broad spectrum of EM problems, including antennas, microstrip circuits, radio frequency (RF) components and biomedical systems, the placement of antennas on electrically large structures, the calculation of scattering (RCS), as well as the investigation of electromagnetic compatibility (EMC) [48].

FEKO offers tools that are tailored to solve the more challenging EM interactions, including dedicated solvers for characteristic mode analysis (CMA) and bi-directional cables coupling. Special formulations are included for efficient simulation of integrated windscreen antennas and antenna arrays [48].

Combined with the multilevel fast multipole method (MLFMM), and true hybridisation of the solvers, FEKO is considered the global market leader for antenna placement analysis [48].

See Figure B.1 which illustrates the numerical analysis techniques in FEKO.

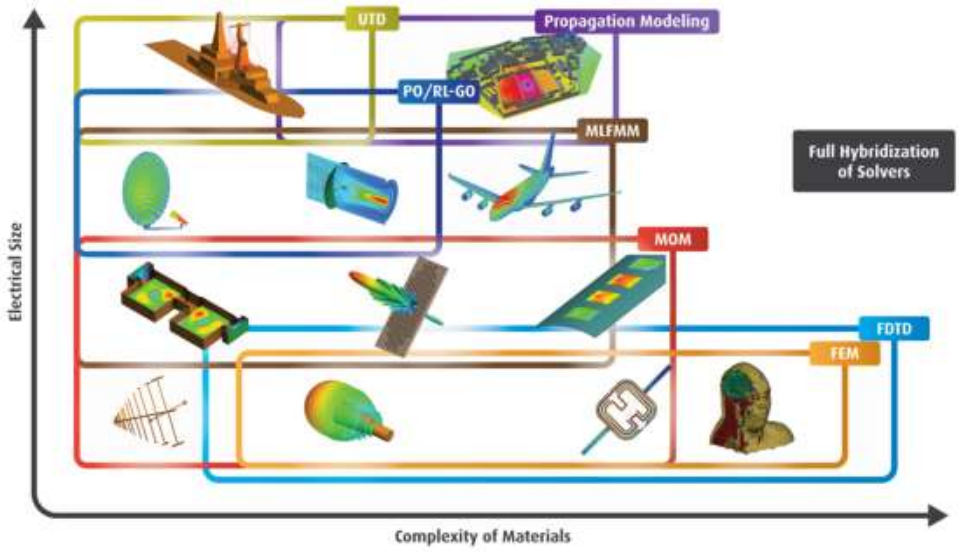

Figure B. 1: Illustration of the numerical analysis techniques in FEKO [48].

Solver Overview

The Solver supports the following solution methods [48].

- Full wave frequency domain solution methods:
  - MoM (method of moments)
  - FEM (finite element method)
  - MLFMM (multilevel fast multipole method)
- Full wave time domain solution methods:
  - FDTD (finite difference time domain)
- Asymptotic solution methods:
  - PO (physical optics)
  - LE-PO (large element physical optics)
  - RL-GO (ray launching geometrical optics)
  - UTD (uniform theory of diffraction)

Appendix C

Detail steps of designing TEM120cm with 200 Ohm aperture impedance in FEKO

I. Creating analytical curve1

The analytical curve equations from section 5.2 design are entered as follows in CADFEKO and note that each of the amplitudes in the Y/V (width) and Z/N (height) are halved since the designed antenna is to be made symmetrical about the X/U and Z/N axis.

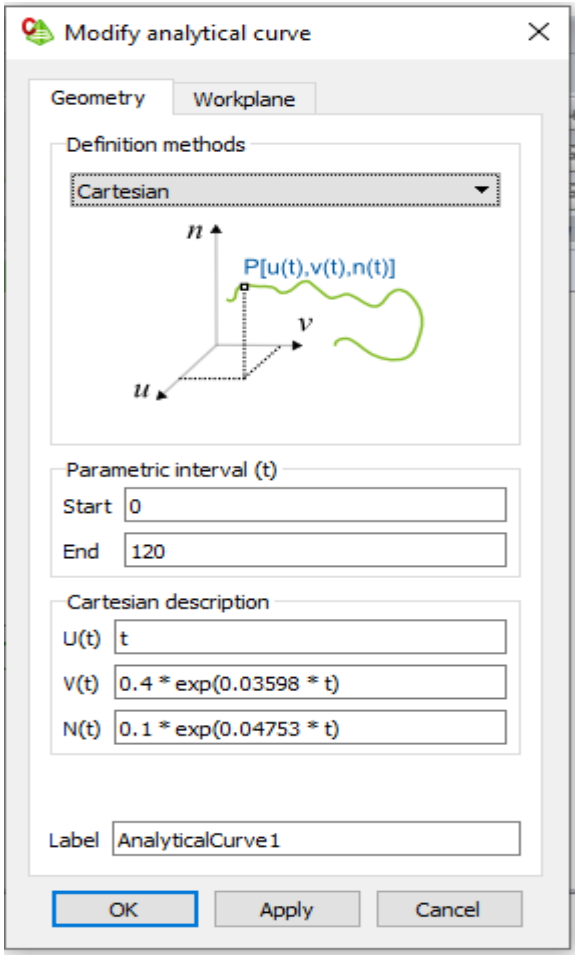

Figure C. 1: Creating analytical curve1 in CADFEKO

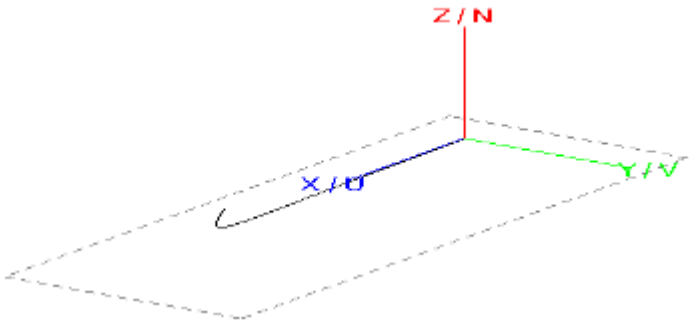

Figure C. 2: Analytical curve1 3D view

II. Creating analytical curve2

The analytical curve equations from section 5.2 design are entered as follows in CADFEKO and note that each of the amplitudes in the Y/V (width) and Z/N (height) are halved since the designed antenna is to be made symmetrical about the X/U and Z/N axis and the negative sign in V(t).

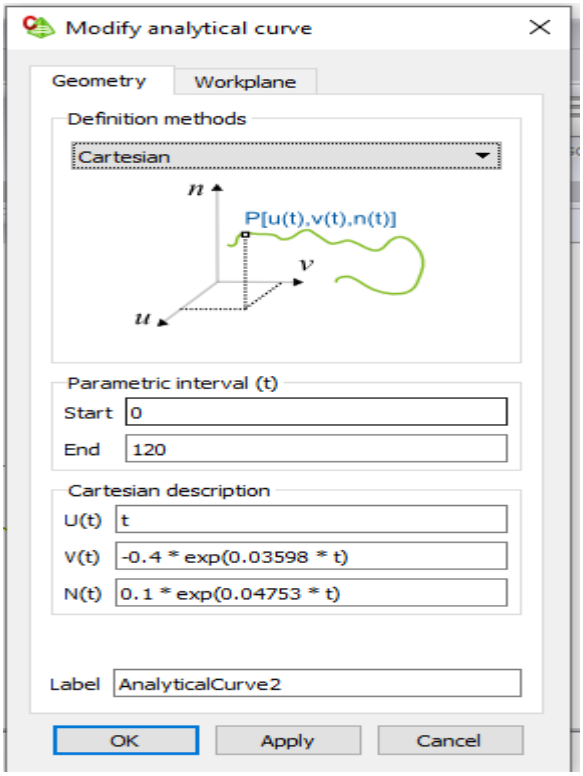

Figure C. 3: Creating analytical curve2 in CADFEKO

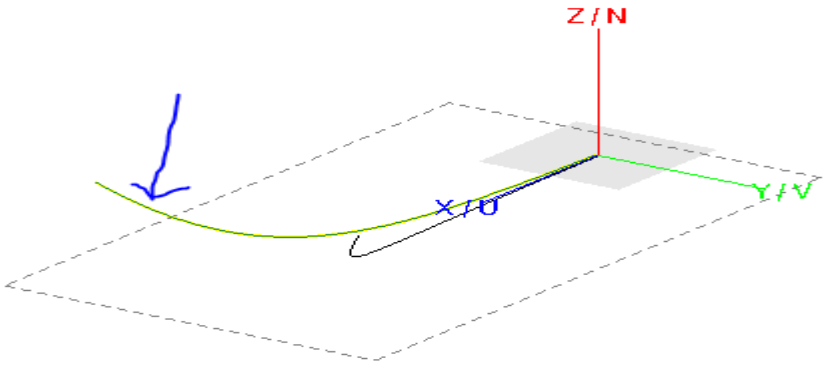

Figure C. 4: Analytical curve2 3D view

III. Lofting analytical curve 1 and 2 to make the upper conductor of the TEM horn

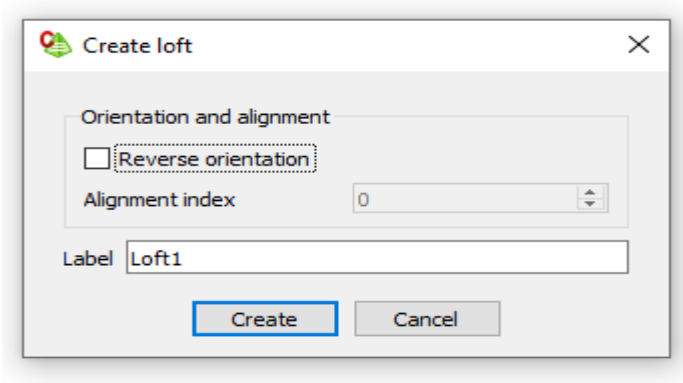

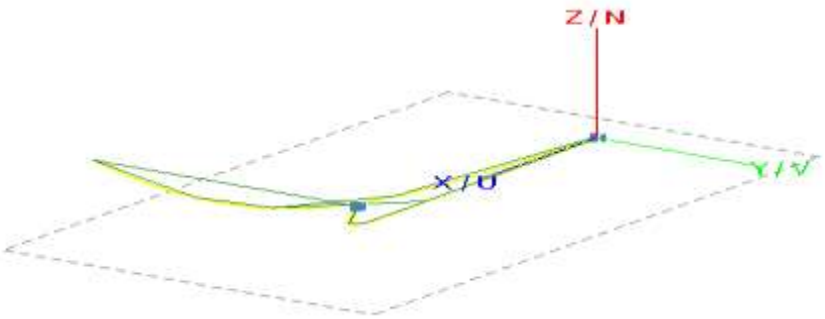

Figure C. 5: Create loft1

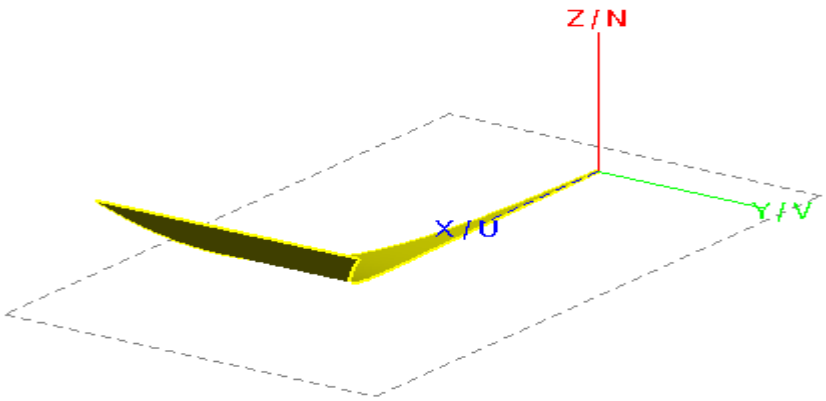

Figure C. 6: Upper conductor of TEM horn

IV. Creating analytical curve3

The analytical curve equations from section 5.2 design are entered as follows in CADFEKO and note that each of the amplitudes in the Y/V (width) and Z/N (height) are halved since the designed antenna is to be made symmetrical about the X/U and Z/N axis and note the negative sign in N(t).

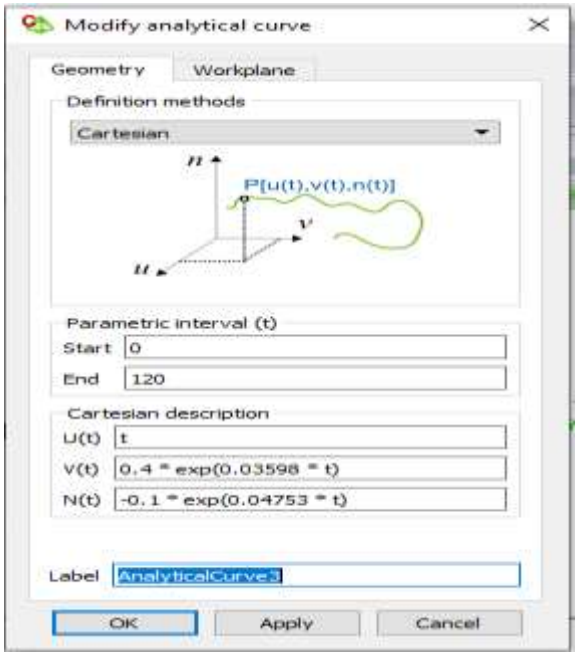

Figure C. 7: Creating analytical curve3 in CADFEKO

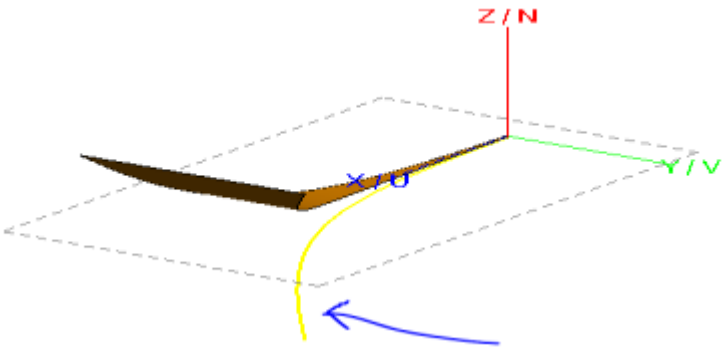

Figure C. 8: Analytical curve3 3D view

V. Creating analytical curve4

The analytical curve equations from section 5.2 design are entered as follows in CADFEKO and note that each of the amplitudes in the Y/V (width) and Z/N (height) are halved since the designed antenna is to be made symmetrical about the X/U and Z/N axis and note the negative sign in V(t) and N(t).

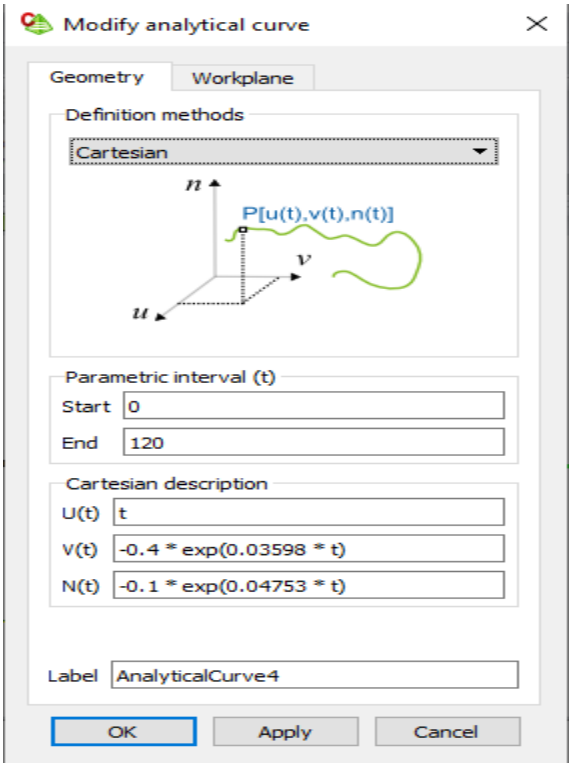

Figure C. 9: Creating analytical curve4 in CADFEKO

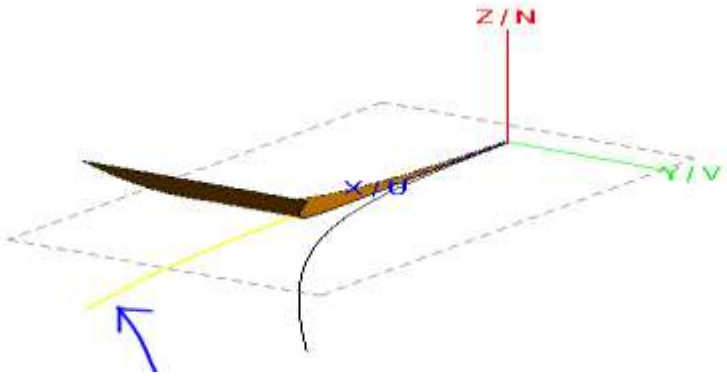

Figure C. 10: Analytical curve4 3D view

VI. Lofting analytical curve 3 and 4 to make the lower conductor of the TEM horn

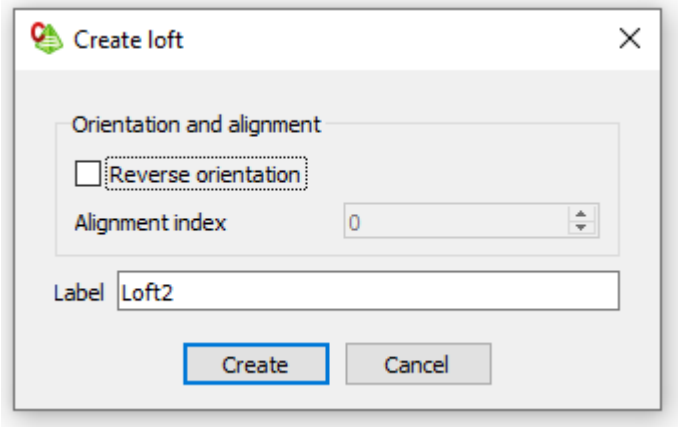

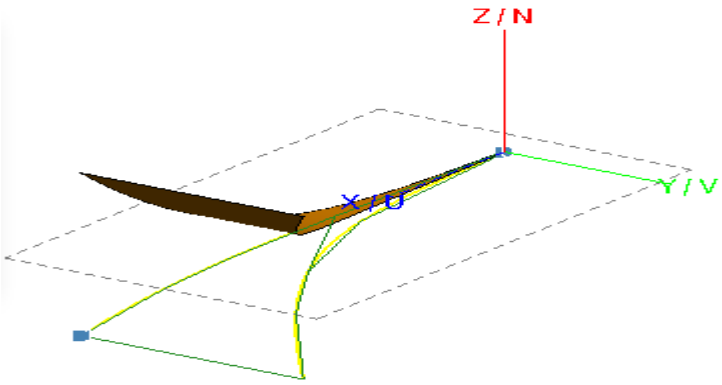

Figure C. 11: Create loft2

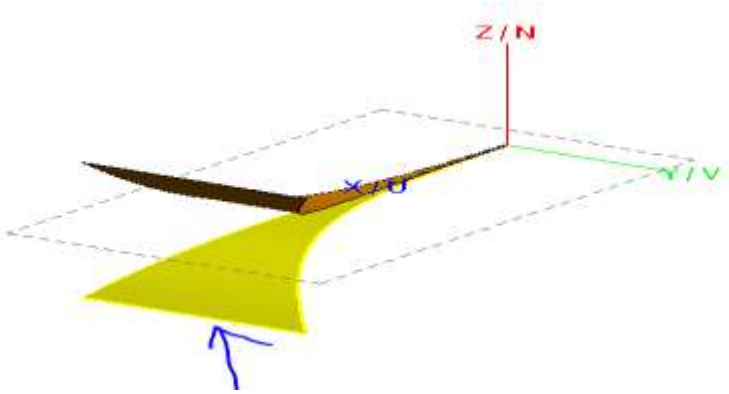

Figure C. 12: Lower conductor of TEM horn

VII. Union upper and lower conductor physically and electrically to make the TEM horn antenna

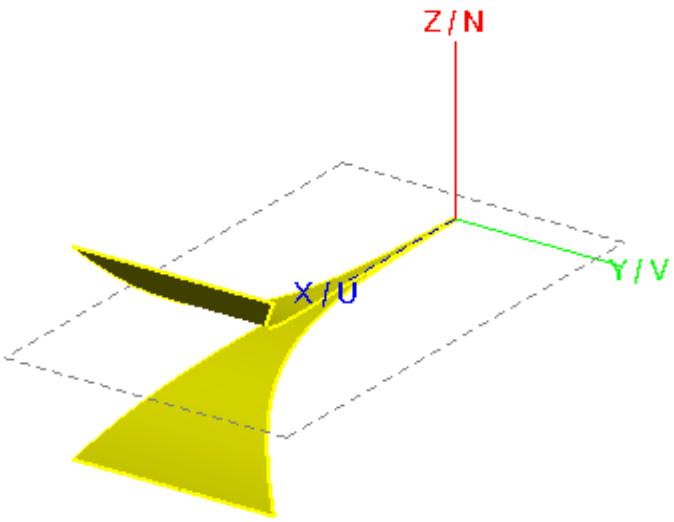

Antenna length along X/U axis (cm) = **120**

Spacing at feed along Z/N axis (cm) = **0.2**

Width at feed along Y/V axis (cm) = **0.8**

Spacing at aperture along Z/N axis (cm) = **60**

Width at aperture along Y/V axis (cm) = **60**

Feed line impedance (Ohm) = **50**

Aperture impedance (Ohm) = **200**

Figure C. 13: TEM120cm with 200 Ohm aperture impedance 3D view (both upper and lower conductor faces are made Perfect Electric Conductor (PEC)